Distinct Microbiomes Underlie Divergent Responses of Methane Emissions from Diverse Wetland soils to Oxygen Shifts

Linta Reji[1,2,3], Jianshu Duan[1], Xinning Zhang[1,2]
[1] Department of Geosciences, Princeton University, NJ
[2] High Meadows Environmental Institute, Princeton University, NJ
[3] Current address: Department of the Geophysical Sciences, The University of Chicago, IL

ORCIDs

Linta Reji: 0000-0002-1337-6782
Jianshu Duan: 0000-0002-3015-1147
Xinning Zhang: 0000-0003-2763-1526

ABSTRACT

The effects of hydrological shifts on wetlands, a globally important source of methane (CH_4), are critical to constraining global CH_4 emissions. Wetland CH_4 emissions are uncertain due to a limited understanding of how hydrologically driven oxygen (O_2) variability affects microbial CH_4 cycling. Transient O_2 exposure has been shown to significantly stimulate anoxic CH_4 production in *Sphagnum* peat from a temperate bog by enriching for polyphenol oxidizers and polysaccharide degraders, enhancing substrate flow toward methanogenesis under subsequent anoxic conditions. To assess whether key structural shifts in soil microbiome operate similarly across wetland types, here we examined the sensitivity of different wetland soils to transient oxygenation. In slurry incubations of *Sphagnum* peat from a minerotrophic fen, and sediments from a freshwater marsh and saltmarsh, we examined temporal shifts in microbiomes using 16S rRNA gene profiling, metagenomics, and metatranscriptomics, coupled with geochemical characterization of the slurries and incubation headspaces (GC-TCD, FTIR, etc.). Oxygenation did not affect anoxic CH_4 emissions from fen-origin peat and freshwater marsh sediments, nor the microbiome structure. Key taxa linked to O_2-stimulated CH_4 emissions in the bog-origin peat were notably rare in the fen-origin peat, supporting microbiome structure as a primary determinant of wetland response to O_2 shifts. In contrast to the freshwater wetlands, saltmarsh geochemistry—particularly pH—and microbiome structure were persistently and significantly altered post-oxygenation, albeit with no significant impact on greenhouse gas emissions. With climate change driving greater O_2 variability in wetlands, our results inform mechanisms of wetland resiliency and highlight microbiome structure as a potential resiliency biomarker.

INTRODUCTION

Wetlands are globally important ecosystems that store ~30% of the terrestrial soil carbon pool (1), despite covering only 5-8% of the land surface (2). Their ability to act as massive carbon sinks stems from the decoupling of primary production and respiration—the typically anoxic waterlogged conditions diminish microbial decomposition of organic matter, promoting carbon

preservation relative to oxic conditions (3–5). This carbon stock is still subject to microbial activity, and as such wetlands contribute significantly to the global emission budgets of potent greenhouse gases, including carbon dioxide (CO_2), nitrous oxide, and in particular, methane (CH_4) (6–8). The rapid increase in atmospheric CH_4 levels observed in recent years has been attributed partly to increasing wetland CH_4 emissions (9–11). Wetlands are among the largest and most uncertain sources of CH_4 to the atmosphere (12). Therefore, accurately accounting for and predicting wetland CH_4 emission trajectories is vital for climate change mitigation.

As wetland biogeochemistry is tightly linked to water table depth (13–15), changes in the frequency and duration of dry-wet cycles and associated oxygen (O_2) and redox shifts will likely cause major changes to wetland biogeochemical cycling (15–17). Anoxic, reducing conditions that prevail during high water table periods can be conducive for methanogenesis (18). In contrast, water table drawdown resulting from droughts or decreased precipitation can oxygenate soils, stimulating methane consumption by aerobic methanotrophs while simultaneously suppressing methanogenesis in oxic layers (19,20). Further complicating the picture, however, is the recent discovery of methane emissions from oxic wetland soils (21–24). This "methane paradox" is generally attributed to anoxic microsites harboring methanogens in otherwise bulk oxic soils (23,24). Oxygen variability, thus, clearly imparts a complex yet strong control on wetland CH_4 fluxes. Deciphering the mechanistic underpinnings of oxygen's roles in wetland CH_4 emissions is a key priority for tracking and predicting global CH_4 emission trajectories across spatio-temporal scales.

Previous experiments on *Sphagnum* peat from a temperate bog showed that transient oxygenation stimulates CH_4 production during subsequent anoxia (25). Mechanistically, O_2 was revealed to play a key role in aromatic oxygenase-driven breakdown of phenolic compounds in peat, thereby removing an O_2-sensitive latch on hydrolytic breakdown of complex sugar polymers (26–28). The resulting surge in labile carbon compounds promoted hydrogen-evolving fermentation and eventually enhanced hydrogenotrophic methanogenesis (25,29). Specific groups of microbes were identified as key mediators of the above processes, namely (i) the proteobacterial genus *Novosphingobium*, which contain O_2-dependent aromatic compound oxygenases and were enriched during the oxic period; (2) the acidobacterial genus *Terracidiphilus* with the ability to break down complex polymers; (3) another acidobacterial genus *Holophaga*, specializing in hydrogen-evolving fermentation of labile carbon compounds; and (4) *Methanobacteria*, which are hydrogenotrophic methanogens (25,29). Transient O_2 exposure of the bog *Sphagnum* peat thus led to a cascade of biogeochemical changes, eventually leading to ~2000-fold higher CH_4 yields compared to continuously anoxic controls (25).

Extrapolating the above observations to different wetland soils is challenging due to their heterogeneous biogeochemistry and microbial dynamics (25,30–32). The observation that aerobic breakdown of phenolics with oxygenation stimulated CH_4 emissions in *Sphagnum* peat (25) is consistent with the enzyme latch theory, which proposes that inhibitory phenolics limit hydrolysis of carbon polymers, thereby promoting carbon storage in anoxic wetland soils (27,33). However, there is variable evidence for the enzyme latch theory, especially with the discovery of anoxic phenolic degradation by various classes of microbes and enzymes (34–38). In iron-rich soils, abiotic reactions during anoxic-oxic oscillations can also lead to phenolic degradation, e.g., (39–43). The enzymatic latch, thus, may not be universally present across wetlands, due to variability

in biogeochemical factors including polyphenol levels and microbiome structure. In addition, variations in terminal electron acceptor pools should shift substrate cascades away from terminal CH_4 production. O_2 variability, therefore, may have limited impact on anoxic CH_4 emissions, depending on wetland soil type.

While previous work on *Sphagnum* peat highlighted specific taxa and enzyme classes as crucial determinants of O_2-stimulated CH_4 emissions (25), the prevalence and importance of these microbial features across wetlands remain unclear. Considering the diverse biogeochemistry of wetlands, we sought to determine the variability in the response of different wetland soils to transient oxygenation. Addressing this question is vital for understanding CH_4 emissions with ongoing and projected changes in the hydrological cycle that are poised to increase the frequency of dry-wet transitions (44,45). Here, we assessed the response of three different wetland soils to brief periods of oxygenation, and compared the results to previous work, in particular to one that found O_2-stimulation of CH_4 emissions in *Sphagnum* peat from a temperate bog (25); and another that did not find stimulation of CH_4 emissions to O_2 shifts in a peat fen (46). The following wetland soils were included in our experiment: (i) *Sphagnum* peat from a forested wetland in the New Jersey (NJ) Pine Barrens; (ii) a mineral-soil freshwater wetland in central NJ; and (iii) a saltmarsh located along the NJ coast. We hypothesized that the enzymatic latch, if present in these wetland soils, will be weakened or eliminated with O_2 exposure, thereby amplifying anoxic CH_4 emissions. Additionally, this effect may be dampened by the presence of alternative terminal electron acceptors for respiration, which divert substrate flow away from methanogenesis under anoxia (47–49). To uncover potential mechanisms underlying wetland soil responses to transient oxygenation, we utilized a controlled laboratory incubation methodology with coupled measurements of microbial and biogeochemical variables.

METHODS

Wetland sample collection, slurry preparation, and incubation set up

Three biogeochemically distinct wetland systems were chosen for sample collection: a *Sphagnum* moss-dominated minerotrophic fen in the New Jersey Pine Barrens, a freshwater marsh in the Charles Rogers Wildlife Refuge in Princeton, NJ, and a saltmarsh in the Swan Point State Natural Area in southern New Jersey coast. At each location, wetland soil was collected from the top ~10 cm beneath the litter/moss layer, if present. In the Pine Barrens, the *Sphagnum* peat fen was located on the banks of Bisphams Mill Creek (39.922 N, 74.591 W), in an area interspersed with Pitch Pines and various shrubs. The freshwater marsh vegetation in the Charles Rogers marshland (40.326 N, 74.659 W) was predominantly composed of cattails. Saltmarsh sediments were collected from the inundated margin of a shallow pond (40.0324 N, 74.0777 W), neighboring patches of *Spartina* grass.

At each location, acid-cleaned UV-irradiated polyethylene bags were filled with peat or sediments and transported on ice back to the laboratory. Site water (~2 L each) was also collected from each location in acid-washed Nalgene bottles. Once in the laboratory, plant roots and litter were removed from the peat/sediments. Slurries were prepared by blending peat/sediments with 0.2 mm-filtered site water in a 1:3 volume ratio (25). The slurries were then flushed with ultrahigh

purity 100% N_2 (Airgas) for 15 minutes, and while continuing to flush with N_2, 60 ml of each slurry was pipetted into acid-washed and autoclaved 160 ml serum bottles. The bottles were immediately closed with butyl rubber stoppers and crimp sealed.

A total of 24 slurry incubations were prepared for each wetland type. Half of these were set up as continuously anoxic controls by flushing with N_2 gas. The remaining half were flushed with Breathing Quality air (21.5 ± 2% O_2 and 78.5 ± 2% N_2; Airgas). After flushing, the bottles were incubated at 20 C, shaking on their side at 150 rpm in the dark. During the oxic period of the incubation, half of the microcosms were kept aerobic by flushing the bottles with Breathing Quality air after every two days. During each flush, the continuously anoxic controls were flushed with 100% N_2 gas. In the long-term incubation experiment, oxic conditions were maintained in the O_2-shifted microcosms for a week, after which all bottles were flushed with 100% N_2, thus establishing anoxic conditions in all. The subsequent anoxic incubations lasted 358 days, during which we tracked differences in biogeochemistry between the treatments. This involved monitoring of headspace gas compositions as well as destructive sampling of triplicate incubations at four timepoints (i.e., days 7, 21, 229 and 365). In a follow-up short-term incubation experiment with the Pine Barrens peat, the O_2-shifted samples were kept aerobic for a month and were made anoxic afterward, with the anoxia lasting 65 days.

Slurry sampling and geochemical measurements

Headspace gas samples were collected periodically to monitor CO_2, CH_4, and H_2 concentrations. Using a sterile Luer lock syringe (BD), 15 ml of the headspace gas sample was collected and stored in pre-evacuated, crimp-sealed amber serum vials. Gas volumes removed from the incubation headspaces were balanced by adding either 100% N_2 or air containing 20% O_2, as appropriate. Final gas concentrations were adjusted for headspace dilution. Concentrations of CH_4, CO_2, and H_2 in the headspace samples were analyzed using a Shimadzu GC-8A gas chromatograph equipped with a Restek ShinCarbon ST column and thermal conductivity detector. Standard curves were prepared using a calibration mixture containing 1% by volume of each target species (Airgas).

On days 7 (end of the oxic period), 21, 229, and 365, three microcosms per treatment were destructively sampled. Slurry samples for DNA/RNA (1 ml each) were aliquoted into duplicate sterile 2 ml cryotubes and stored at -80 C until extractions. 100 µL each of the slurry was used for determining ferrous ion concentrations. Another 1 ml each was used for measuring dry weight and organic matter content. Remaining slurry was centrifuged for 20 minutes at 10,000 rpm to separate out the solid and liquid fractions. The supernatant was 0.2 µm-filtered and aliquoted into clean serum vials (acid washed and combusted) for dissolved organic carbon, volatile fatty acids (VFAs), and phenolic content analyses. Solid fractions were saved at -20 C for nutrient analyses (total carbon, total nitrogen, and anions).

Slurry pH was determined by using a waterproof pH meter (Oakton) and immersing the electrode in 1 ml of the slurry sample aliquoted to a sterile conical tube (Corning). Dry weight was determined by oven-drying the slurry samples in ceramic crucibles at 105 C to a constant weight. Percent organic matter was estimated using the loss-on-ignition method, by combusting dried slurry samples at 505 C for 3 hours. Ferrous ion and total iron concentrations were measured using

the Ferrozine colorimetric assay. Standard curves were prepared by dissolving ferrous sulfate in 0.5 N hydrochloric acid. Water-extractable phenolics in the slurry supernatant was measured using the Folin-Ciocalteu colorimetric assay, using a standard curve prepared using gallic acid. Concentrations were calculated as mg/ml gallic acid equivalent. Acetate concentrations were measured on an Agilent HPLC equipped with Bio-Rad Aminex HPX-87H (300 mm × 7. 8 mm) and a DAD detector.

Infrared spectra of filtered supernatants were collected on a Bruker VERTEX 80v spectrometer equipped with a liquid-nitrogen-cooled mercury cadmium telluride (MCT) detector. Aliquots of 1 µL solution were added to the surface of a diamond ATR (attenuated total reflectance) crystal mounted on a Golden Gate ATR sample stage (Specac), and the solution was dried under moisture- and CO_2-free air (Spectra 30 FTIR purge gas generator, Parker Balston). This step was repeated 5 times until a thin film was formed. The sample spectrum was measured as the average of 2000 scans at a scan velocity of 80 kHz with a 5 mm aperture setting. A blank spectrum was collected immediately before each sample spectrum and subtracted. All spectra were collected at 4 cm^{-1} resolution. Baseline corrections were performed on the ATR spectra using the OPUS software (Bruker). IR spectra were imported to R (v4.2) and analyzed using the package ChemoSpec (v6.1.10; (50)).

All statistical analyses and plotting of the geochemical datasets were carried out in R (v4.2), using various packages, including stats (v4.4.1; (51)) and tidyverse (v2.0.0; (52)) core packages and add-ons.

Nucleic acid extractions, 16S rRNA gene sequencing, and microbiome analyses

Total RNA and DNA were co-extracted from the slurry samples (Table S1) by combining the RNeasy PowerSoil Total RNA kit with the RNeasy PowerSoil DNA Elution kit (Qiagen), using manufacturer's protocols. Nucleic acid concentrations were measured using Qubit 4 Fluorometer (Thermo Fisher), and their quality was assessed using a NanoDrop spectrophotometer (Thermo Fisher). Samples were stored at -80C for later analyses.

The V4 region of the 16S rRNA gene was sequenced using Illumina MiSeq at the Princeton Genomics Core facility. Demultiplexed raw reads were primer trimmed using Cutadapt (v1.18; 29), and then, quality filtered, denoised, and merged with DADA2 (v1.26; (54)) in R (v4.2.1; (51)) to identify Amplicon Sequence Variants (ASVs). ASVs were assigned taxonomy using the Silva database (r138.1; (55)). DADA2 outputs, including taxonomic assignments and ASV read counts, were imported into PhyloSeq (v1.38; (56)) for further analyses (all performed in R v4.1.2). Eukaryotic, including mitochondrial and chloroplast, sequences were filtered out. During pre-processing, rarefaction curves were calculated separately for each wetland type to determine outliers to discard from analyses. As a result, samples without a plateauing rarefaction curve were discarded. The final pre-processed dataset included 28 Pine Barrens peat samples, 22 freshwater marsh samples, and 20 saltmarsh samples, including several technical replicates. All analyses were performed separately for each wetland type. Alpha diversity (Chao1 and Inverse Simpson) was measured using the plot_richness function in Phyloseq. The tax_fix function in microViz (v0.10.2; (57)) was used to fix missing values in the taxonomy tables. Bar plots of relative abundances were then obtained using the microshades (v1.10; (58)) package. Differential abundance testing was

performed at the genus level by using Analysis of Composition of Microbiomes with Bias Correction (59,60) as implemented in the ANCOMBC package (v1.4).

Metagenome and metatranscriptome sequencing and analyses

Nucleic acid samples passing the required quantity and quality thresholds (minimum yield of 0.5 μg and acceptable purity ratios) were used for metagenomic and metatranscriptomic sequencing. For each wetland type, one of the three replicates for each treatment across timepoints were selected for metagenome sequencing. This amounted to 9 metagenomes each per wetland type (i.e., initial T0 sample, and 4 timepoints each for the O_2-shifted and continuously anoxic treatments). The timepoints correspond to days 0, 7 (end of the oxic period), 21, 229, and 365. Since the saltmarsh samples from later timepoints did not yield good quality DNA (Table S1), only 5 metagenomes were obtained for these, corresponding to time zero, and 2 timepoints each for the O_2-shifted and continuously anoxic incubations. Metatranscriptomes were obtained for several of the PB peat and saltmarsh incubations, spanning two timepoints per treatment.

Paired-end sequences were obtained using the Illumina NovaSeq platform (S1 300nt flowcell) at the Princeton Genomic Core facility. Demultiplexed metagenomic reads were quality filtered using FastQC (v0.11.9; (61)) and Trimmomatic (v0.39; (62)). Anvi'o (v7.1; (63)) was used for assembly, mapping, and contig functional assignments. Metagenomes for each wetland type were co-assembled using MEGAHIT (--min-contig-len 1000; v1.2.9; (64,65)). Bowtie 2 (v2.3.5; (66)) was used to map reads to the assembled contigs. Contig functional annotations were obtained by using the functions "anvi-run-hmms" and "anvi-run-ncbi-cogs". Demultiplexed metatranscriptomes were quality filtered using FastQC (v0.11.9; (61)) and cutadapt (v2.10; (53)). QC-filtered reads were mapped to co-assembled metagenomic contigs for each wetland type. Mapping was performed using bowtie2 (v2.3.5; (66)) in Anvi'o (v7.1; (63)). Metagenome contigs were binned using MetaBAT 2 (v1.12.1; (67)), MaxBin 2 (v2.2.7; (68)), and CONCOCT (v1.1.0; (69)). Bin refinement was carried out using the bin_refinement module in MetaWRAP (v1.2; (70)). Prodigal (v2.6.3; (71)) was used to obtain amino acid sequences of gene calls for each bin. These were uploaded to the GhostKoala server (72) to obtain KO annotations. Refined bins along with the corresponding KO annotations were exported into the merged Anvi'o profile as a collection. Relative distributions of assembled genomes and predicted functions across the metagenomes and metatranscriptomes were estimated using the "anvi-summarize" function. Additional functional annotations for the assembled genomes were obtained via DRAM (73) and RASTtk (74) within the KBase platform (75).

RESULTS AND DISCUSSION

Oxygen controls complex carbon degradation in wetland soils directly via acting as a terminal electron acceptor for aerobic respiration, and indirectly by regulating the activity of microbial exoenzymes. Microbes produce diverse classes of exoenzymes to facilitate the breakdown of complex wetland carbon, primarily composed of polysaccharides (e.g., cellulose, hemicellulose) and polyphenolics (e.g., lignin, tannins) (25,76). Polysaccharide hydrolysis, which does not directly depend on O_2, generates simpler oligomers that are readily respired or fermented. Polyphenolics degradation, in contrast, is generally O_2-dependent as aromatic oxidases, commonly

termed "phenol oxidases", directly use O_2 as a co-substrate for the oxygenation reaction (25-27). Anoxic conditions, therefore, typically lead to polyphenol accumulation. However, recent genomic and geochemical evidence suggests active polyphenol breakdown even under anoxia (38,77). The magnitude of these fluxes under different conditions and their relative importance for wetland carbon budgets remain to be ascertained. In the absence of significant removal, accumulating polyphenols can curtail polysaccharide hydrolysis by binding to hydrolase enzymes, and thus, effectively resulting in an "enzyme latch" on carbon degradation (25-27). This "enzyme latch" hypothesis has been proposed as a mechanism critical for carbon storage in wetlands (25-27). Many studies, however, have found contrasting evidence for the existence or strength of such a latch in various wetland systems (34,35,78), suggesting underexplored complexity in using the latch hypothesis in explaining the fate of carbon in wetlands.

Previous experiments on *Sphagnum* peat from a peat bog in Ward Reservation, MA (herein "Ward peat") revealed that an enzyme latch likely existed in this system as oxygenation significantly enhanced anoxic CH_4 production (25). Geochemical and microbial data aided in unraveling the underlying complex mechanisms: during the oxic period, aerobic respiration accelerated the breakdown of complex aromatic compounds, which removed the O_2-sensitive latch on hydrolytic enzyme activity, thereby promoting the degradation of large polymeric compounds. This generated labile carbon compounds that were readily fermented during the subsequent anoxic period, increasing substrate flux towards methanogenesis (25,29). Since phenolic compounds and carbohydrate polymers comprise the majority of organic matter in typical *Sphagnum* peat (79–82), processes such as transient oxygenation that can accelerate the breakdown of these compounds (34–38) would greatly mobilize the carbon stock and enhance CH_4 emissions.

To probe the presence of an "enzyme latch" in diverse wetland soils and to assess their response to transient oxygenation, we performed a laboratory incubation experiment using wetland soils from a minerotrophic peat fen, a freshwater marsh, and a saltmarsh. Our study design utilizing controlled incubations of peats and wetland soils allowed a mechanistic assessment of (i) the heterogeneous response of wetland CH_4 and CO_2 emissions to O_2 shifts, and (ii) the microbial and geochemical determinants of wetland resiliency under redox alterations.

Fen-origin PB peat geochemistry resilient to the O_2 *shift*

Headspace gases

Transient O_2 exposure did not stimulate CH_4 emissions in fen-origin *Sphagnum* peat from the New Jersey Pine Barrens (herein "PB peat"), in contrast to the bog-derived Ward peat incubations (25), highlighting heterogeneous responses of peat types to O_2 shifts (Fig. 1a,b vs. c). Regardless of the duration of the oxic period (1 week versus 4 weeks), O_2 exposure did not stimulate anoxic CH_4 production in PB peat (Fig. 1a, S3). Like in Ward peat, oxygenation delayed the onset of methanogenesis: CH_4 was detected in the O_2-shifted incubation headspaces only after ~4 weeks of anoxia following the oxic period (Fig. 1a). In comparison, within a week of anoxic incubations, detectable CH_4 was present in the continuously anoxic control incubations (Fig. 1a). As the experiment progressed, overall CH_4 yields were similar between the O_2-shifted and continuously anoxic PB peat incubations (Fig. 1a), underscoring the absence of any O_2-stimulated enhancement of methanogenesis. In comparison, the O_2-shifted Ward peat incubations generated up to >1000-fold higher amounts of CH_4 compared to continuously anoxic controls (Fig. 1b),

clearly demonstrating a key role for O_2 in peat carbon degradation under anoxic conditions in this system.

O_2 exposition also led to higher anoxic CO_2 emissions in Ward peat, but not in PB peat (Fig. 1b, 1c). In the latter, a sharp increase in CO_2 emissions was observed initially upon oxygenation (Fig. 1a, 1b), indicating aerobic respiratory breakdown of peat organic carbon. The O_2-shifted PB peat incubations yielded ~15-fold higher amounts of CO_2 during the oxic period compared to the anoxic controls (Fig. 1b). Following the onset of anoxia, the two treatments were largely similar in CO_2 emissions, indicating that any O_2-induced change in CO_2-forming metabolism was short-lived (Fig. 1a, 1b). This was in stark contrast to the Ward peat, which showed much higher (~20- to 150-fold) CO_2 emissions in the O_2-shifted incubations compared to anoxic controls long into the anoxic period following the O_2 shift (Fig. 1c). These observations indicate that the brief O_2 exposure enhanced CO_2-forming carbon mineralization in Ward peat in addition to promoting methanogenesis, likely by increasing the flux and availability of labile compounds for microbial degradation which persisted into the anoxic period. Such an effect appears to be absent in the PB peat, where O_2-mediated CO_2-forming respiration during the oxic period likely did not yield a similar influx of labile C for further anoxic degradation.

The headspace hydrogen (H_2) evolution trajectories provide further evidence for the lack of O_2 stimulation of anoxic metabolism (specifically fermentation) in PB peat compared to Ward peat. Both the O_2-shifted and continuously anoxic PB peat incubations showed high levels of H_2 in the headspace during the first three weeks of incubation (Fig. 1a). H_2 levels dropped below the detection limit by week 3 and remained undetectable for the remainder of the experiment (Fig. 1a). In contrast, significant amounts of H_2 were detected in the Ward peat incubation headspaces even at the final incubation timepoint (day 232, 134 days anoxic; Fig. S1; ref. 24). In addition, acetate, another key product of microbial fermentation, accumulated at millimolar levels in the Ward peat (up to ~2.5 mM in O_2-shifted Ward peat and ~7 mM in the anoxic controls; ref. 24). In contrast, no measurable acetate was detected in the PB peat incubations at any timepoint during the incubation (detection limit 560 μM).

Aqueous phase geochemistry

O_2 exposure further led to a decline in pH and Fe(II) concentrations in the PB peat incubations, which coincided with a sharp increase in sulfate (SO_4^{2-}) levels (Fig. 2), likely derived from the oxidation of reduced organosulfur compounds that can be abundant in peat (83) or iron-sulfides (84,85). Fe(II) and SO_4^{2-} levels were reestablished to prior values upon making the incubations anoxic (Fig. 2), potentially indicating the coupled effect of microbial transformations such as sulfate reduction and the regeneration of reduced iron- and sulfur-compounds. At least at the very beginning of the anoxic period in the O_2-shifted peat, SO_4^{2-} and Fe(III) may have served as alternative electron acceptors for microbes. However, SO_4^{2-} levels remained well-below the limiting concentration for microbial sulfate reduction (300 mM; (83,86)), and therefore, the importance of cryptic microbial sulfate reduction in PB peat remains unclear.

To sum up the geochemical observations, carbon degradation pathways in PB peat appeared to be largely unaffected by the O_2 shift, likely due to a weak enzymatic latch in this peat. This is further evidenced by the lack of measurable phenolics in the initial PB peat sample (Fig. 2). Total phenolics were ~2- to 5-fold higher in the anoxic controls compared to the O_2-shifted

samples on day 7 and 21 (Fig. 2), indicating O_2-mediated breakdown of polyphenols in the O_2-shifted samples. Following the oxic period, FTIR data indicated the mobilization of small organic molecules, including aromatics (C=C at 1627, 1594, and 1493 cm^{-1}), amides (amides I and II bands at 1655 and 1579 cm^{-1}, respectively), and aliphatics (C-H between 2700 and 3000 cm^{-1}), which were absent in the anoxic controls and diminished at later timepoints, suggesting microbial consumption (Fig. S2). The anoxic and O_2-shifted samples had largely similar IR spectra at later timepoints during anoxia (Fig. S2), suggesting a reset of soluble organic matter composition following oxygenation. This contrasts starkly with the Ward peat, where FT-ICR-MS data revealed major changes in organic matter composition, notably significant O_2-enhanced removal of aromatic compounds (24).

Overall, geochemical measurements point to distinct controls on microbial carbon metabolism in the two peats. Even a relatively short period of O_2 pre-exposure was sufficient to enhance CH_4 release in Ward peat (e.g., ~55-fold increase in anoxic CH_4 emissions following a week of O_2 exposure; 24). The apparent absence of such an effect of O_2 shift in PB peat (Fig. 1a), even with a longer period of O_2 pre-exposure of 30 days (Fig. S3) suggests fundamentally different controls on microbial metabolisms and carbon cycling in these two *Sphagnum* peats. In addition, the lack of accumulation of fermentation byproducts in PB peat indicate either a tight coupling of fermentation with methanogenesis or alternative anaerobic respiration of organic matter in this peat. The increase in sulfate concentrations in PB peat upon O_2 exposure (Fig. 2a) suggest the possibility of sulfate reduction as an alternative respiratory metabolism during anoxia in this peat.

Fen-origin PB peat microbiome largely resilient to the O_2 *shift*

Microbial community structure and its response to the O_2 shift in the fen-origin PB peat contrasted strongly with that of Ward peat. O_2-stimulation led to significant changes in the Ward peat microbiome (24, 28). The PB peat microbiome, in contrast, was largely resilient to the O_2 shift, as the two treatments were similar in community composition throughout the experiment (Fig. 3a). As the experiment progressed, the PB microbiome shifted from a community dominated by *Proteobacteria* and *Acidobacteriota* to one dominated by *Bacteroidota* (Fig. 3a). These changes were, however, independent of the O_2 shift, as they were consistent between anoxic and O_2-shifted samples.

Notable taxa and functions associated with a weaker "latch" in PB peat

Key taxa observed to be vital players in the O_2-stimulated CH_4 emissions in Ward peat were noticeably rare in PB peat. In Ward peat, three major microbial groups were identified as key players in the O_2 response: *Novosphingobium*, an alphaprotebacterial genus harboring aromatic oxidases, Acidobacteria (specifically, the genera *Holophaga* and *Terracidiphilus*) capable of polysaccharide hydrolysis and fermentation, and *Methanobacterium*, a methanogenic genus of the phylum Euryarchaeota (25). *Novosphingobium* were significantly enriched in the O_2-shifted Ward peat, comprising up to 80% of the 16S rRNA gene amplicons during the oxic period. Similarly, *Acidobacteria* were enriched under anoxia, comprising >50% of the community (24, 28). These taxa were relatively rare (overall abundance <5% of the community) in the PB peat microbiome (Fig. 3a, S4). The relative abundance of *Novosphingobium* indeed increased in PB peat immediately following the O_2 exposure, however, they still only comprised <2% of the total

community (Fig. S4). *Holophaga* were present throughout the incubation period in PB peat although they constituted a very small proportion of the community (i.e., up to 5% relative abundance in PB peat versus ~50% in Ward peat; Fig. S4). Also, unlike in the Ward peat incubations, *Holophaga* abundances did not vary between O_2 treatments in PB peat. Similarly, the primary methanogen in the community, *Methanobacterium*, also did not increase in abundance during anoxia in O_2-shifted PB peat unlike in Ward peat (Fig. 3a).

While O_2 exposure did not alter the PB peat microbiome as drastically as it did the Ward peat microbiome, subtle yet short-lived compositional changes still followed the oxygenation period. There was a sharp increase in community alpha diversity with O_2 exposure (i.e., measured as the number of observed amplicon sequence variants or ASVs; Fig. S5), as diverse microbes likely exploited the new niche for aerobic respiration. This effect was relatively short-lived as the O_2-shifted samples progressively became less diverse over time, and significantly lower than anoxic controls at later timepoints (Fig. S5; Wilcoxon Rank Sum test with FDR adjusted p-values $< 2e\text{-}16$ for all). In comparison, the continuously anoxic controls showed largely invariable ASV richness throughout the experiment (Fig. S5). ANCOM differential abundance testing uncovered 24 ASVs in the PB peat microbiome as differentially abundant between the O_2-shifted and continuously anoxic treatments (q-value < 0.001; Fig. S6a). However, most of these ASVs had log Fold Change values < 1 (with the maximum being 1.5; Fig. S6a), suggesting that the abundance differentials were rather small. Both treatments showed a reduction in community evenness over time (as measured using the Inverse Simpson index), suggesting an increasingly uneven distribution of microbial populations among the ASVs (Fig. S5). In other words, while the overall richness of the communities decreased over time, certain ASVs (i.e., "species"-level lineages) became increasingly dominant. Overall, the PB peat microbiome was largely resistant to the O_2 shift, despite some differences in the relative abundances of ASV- ("species-") level sub-lineages across the O_2 treatments (Fig. S5, S6). Temporal changes in community composition in the PB peat microbiome (Fig. 3a) are thus, likely more reflective of the "bottle effect", which results from changes in the quality and quantity of metabolic substrates over time. These patterns contrast sharply with Ward peat, where the microbiome composition varied significantly not only across timepoints but also between the O_2 treatments (24, 28).

Consistent with the microbiome composition data, comparisons of key functional profiles between the O_2 treatments also highlighted the difference between the two peats in their response to transient O_2 exposure: aromatic oxygenases (phenol hydroxylases and catechol dioxygenases) found to be enriched during the oxic period in Ward peat (25) were of notably low abundance in the PB peat metagenomes and metatranscriptomes and did not respond to the O_2 shift (Fig. 3b, 3c). This agrees with the FTIR data showing minimal changes in aromatic compound transformations post oxygenation and a modest accumulation of likely oxidized aromatics in the aqueous phase following oxygenation (Fig. S2). Indicating potential importance of alternative electron acceptors in PB peat, sulfite reductase (DsrAB) transcripts were relatively more enriched in the O_2-shifted PB peat than in the anoxic controls (Fig. 3b, 3c), which coincided with the higher levels of sulfate measured in the O_2-shifted samples at the end of the oxic period (day 7; Fig. 2). Methanogenesis, as expected, was more enriched in the continuously anoxic controls compared to the O_2-shifted samples (using the marker gene methyl coenzyme M reductase, *mcrA*; Fig. 3b, 3c).

Assembling metagenome contigs into draft genomes (i.e., MAGs) allowed a more nuanced look at the differentially abundant and active lineages across treatments and timepoints in PB peat. We obtained 72 medium- to high-quality MAGs (i.e., > 70% complete; <10% contamination) from the metagenomes (Table S2). DESeq differential abundance testing revealed 7 MAGs as being differentially abundant between O_2-shifted and anoxic PB peat (Fig. 3d), and 19 as differentially active across treatments (i.e., differential read recruitment in the metatranscriptomes; Fig. 3e).

Both the metagenome and metatranscriptome abundance profiles indicated that lineages within major phyla respond differentially to the O_2 shift, suggesting diverging niche adaptations and metabolic strategies among related organisms. Among the six *Bacteroidota* MAGs identified as differentially abundant between treatments in the metagenomes, only one was differentially enriched in O_2-shifted samples while the remaining five were relatively more abundant in the anoxic controls (Fig. 3d). Functional comparisons did not reveal any discernable metabolic features between these MAGs. A *Pseudomonadota* MAG bin_23 (novel genus within family *Spongiibacteraceae*) was relatively more abundant in both the PB peat metagenomes and metatranscriptomes during the oxic period (day 7; Fig. 3d,e). In addition to the aerobic respiration machinery, this MAG harbored pathways for O_2-dependent degradation of aromatic compounds. Among the differentially active MAGs, although most appear to be facultatively anaerobic heterotrophs, a few stood out in terms of alternative respiration capabilities. Specifically, bin_31 (*Pseudomonadota* genus *Usitatibacter*) and bin_64 (*Acidobacteriota* genus Fen-183), which were differentially abundant in the O_2-shifted PB peat metatranscriptomes (Fig. 3e), have the potential for sulfate reduction. Bin_31 additionally has the potential for iron oxidation (Table S3). Their heightened activity during the oxic period thus coincides with the initial decrease in Fe (II) and surge in sulfate upon oxygenation of PB peat (Fig. 2).

Freshwater marsh and saltmarsh responses to O_2 *shift*

To compare the sensitivity of different types of wetlands to O_2 shifts, we repeated the incubation experiments with sediments collected from a freshwater marsh (herein "FW marsh") and saltmarsh. CH_4 was detected in the FW marsh incubation headspaces only after 3 weeks of anoxic incubation (compared to 1-week of anoxic incubation of PB peat). CH_4 yield was generally 1 order of magnitude lower than in PB peat (Fig. 4a and 1a). CH_4 production in the O_2-shifted FW marsh samples was initially lower compared to the continuously anoxic controls; however, over time, similar quantities of CH_4 were measured in both treatment headspaces (Fig. 4). Thus, similar to PB peat, transient O_2 exposure had no significant effect on CH_4 release during the subsequent anoxic period in FW marsh either (Fig. 4a). CO_2 yields in the FW marsh incubations were also several folds lower compared to PB peat incubations (Fig. 4a and Fig. 1a). Prior O_2 exposure led to slightly higher CO_2 concentrations in the FW marsh incubations compared to anoxic controls, but the difference was increasingly insignificant over time (Fig. 4a).

In contrast to both PB peat and FW marsh, the O_2-shifted saltmarsh incubations, on average, released higher amounts of CO_2 (1.6- to 3.8-fold) during the anoxic period than continuously anoxic controls as the incubations progressed (Fig. 4b). Interestingly, this difference was only observed with long (>6 weeks) anoxic incubation of the O_2-shifted saltmarsh samples; during and immediately following the oxic period, both treatments released similar amounts of CO_2 (Fig. 4b). Relatively small amounts of CH_4 were detected in the headspaces of a few of the

saltmarsh incubations at a couple of timepoints during the anoxic phase (Fig. 4b); however, there appeared to have been active turnover of this CH_4 as the levels dropped below detection at later timepoints (Fig. 4b).

Measured geochemical properties of the slurry changed quite significantly upon oxygenation in all three wetland types (Fig. 4c, S7). These changes, however, were rather short-lived in both the PB peat and FW marsh as the O_2-shifted and continuously anoxic samples converged over time (Fig. 2, 4c, Fig. S7). Saltmarsh geochemistry, on the other hand, was more persistently altered upon O_2 exposure: samples in the two treatments continued to diverge in their measured geochemical properties even after several months of anoxic incubations (Fig. 4c, S7). This pointed to more persistent changes in saltmarsh geochemistry upon oxygenation compared to the other two wetland types, likely driven by the significant drop in pH (~6.5 in the initial sample to 4 in the O_2-shifted sample; Fig. S7), and approximately twofold increase in sulfate levels (Fig. S7).

Microbiome responses to O_2 *shifts in the freshwater marsh and saltmarsh incubations*

Microbiome response to O_2 shift in the FW marsh was strikingly similar to that in PB peat, with both communities transitioning form Proteobacteria-dominated to Bacteroidota-dominated over time (Fig. 5a). As in the case of PB peat, these changes did not reflect any effect of the O_2-pretreatment in FW marsh either, as O_2-shifted and anoxic samples were compositionally similar across timepoints (Fig. 5a). These observations further align with the minimal changes in geochemistry upon oxygenation (i.e., no significant difference in trace gas emissions between the two treatments and the lack of persistent changes in sediment geochemistry; Fig. 4a, 4c).

The saltmarsh microbiome, in contrast, changed significantly upon O_2-addition (Fig. 5b), as would be expected based on the notably different geochemical properties of the anoxic controls and O_2-shifted samples (Fig. 4c). The anoxic controls were dominated by *Desulfobacterota* and *Bacteroidota* throughout the incubation period, with little compositional changes with time (Fig. 5b). The O_2-shifted samples were differentially enriched in *Proteobacteria* and specific lineages of *Bacteroidota*, with *Firmicutes* becoming abundant towards the final timepoints (Fig. 5b). In particular, *the genus Maritimimonas* (phylum *Bacteroidota*) significantly increased in relative abundance upon oxygenation and remained dominant into early phase of the anoxic period (Fig. 5b). With prolonged anoxia, a different *Bacteroidota* genus *Lutibacter* became increasingly more abundant in the O_2-shifted samples, along with the *Firmicutes* family *Izemoplasmataeceae* (Fig 5b). In contrast to PB peat, much higher log Fold Change values (up to 4.5 and -3.5) were observed for the differentially abundant ASVs in the saltmarsh incubations (Fig. S6c). Thus, the O_2-shifted and continuously anoxic saltmarsh microbiomes remained compositionally dissimilar throughout the incubation period (Fig. 5b), aligning with the persistent changes in geochemistry brought about by O_2 exposition (Fig. 4c).

Several phylogenetically novel MAGs were obtained from the saltmarsh metagenomes, including one that was classified as a new phylum-level lineage (Table S2). Aligning with the community composition patterns observed for the ASV data, many of the MAGs were conspicuously differentially abundant across the two treatments (Fig. 5c, 5d). The altered geochemistry persisting long after O_2 exposition in the saltmarsh (Fig. 4c) likely promoted

differential enrichment of microbial taxa in these incubations. Ecological or biogeochemical consequences of these observations, especially in field settings, remain to be examined.

Broader implications

Hydrological shifts leading to O_2 variability are a primary control on the dynamic nature of wetland greenhouse gas emissions. The specific mechanistic underpinnings of this control remain challenging to decipher, in particular, the effect of O_2 shifts on wetland microbial biogeochemistry, impeding our ability to accurately account for wetland contributions to climate-active trace gas emissions.

Microbial and geochemical factors regulating wetland response to O_2 *shifts.*

Several studies have reported accelerated carbon degradation (i.e., CO_2 emissions) in response to droughts or redox shifts in wetlands (13,25,33). Such observations have typically been attributed to O_2-stimulated breakdown of complex carbon compounds (13,25). Our results, however, highlight the heterogeneity in wetland responses to O_2 shifts, even in peat dominated by the same plant genus, *Sphagnum*.

The stark contrast between the Ward *Sphagnum* peat and the PB forest *Sphagnum* peat reveal the variable effects of O_2 shifts on peat CH_4 emissions. In the Ward peat, geochemical and microbial data indicated a key role of O_2 in promoting the degradation of complex aromatic and polymeric carbon, promoting H_2-, acetate-, and CO_2-evolving fermentation, and eventually leading to a surge in methanogenesis (Fig. 6). No such patterns were observed in PB peat as exemplified by several geochemical and microbial measurements, namely, (i) only minor compositional shifts in the microbiome with the O_2 shift (Fig. 3), (ii) no enrichment of aromatic carbon degraders and associated enzymes (Fig. 3b, 3c), and (iii) the lack of accumulation of fermentation byproducts (H_2 and acetate). While hydrogenotrophic methanogenesis seemed to be the dominant methanogenic pathway in both peats (since *Methanobacteria* were the dominant methanogens in both cases), O_2 exposure did not result in enhanced substrate flow towards methanogenesis in PB peat unlike in Ward peat. Overall, microbial carbon degradation appears to have followed significantly different routes in the two peat types. These differences may arise from a variety of factors, including differences in the initial microbiome composition, presence of alternative electron acceptors, and the larger ecological and environmental context of each peat system.

The environmental context of each peat system potentially exerts a major control on CH_4 biogeochemistry: while the Ward peat originated from a peat bog, the PB peat originated from a *Sphagnum*-dominated minerotrophic fen located along the banks of a freshwater creek. Given its proximity to the creek, the PB peat system likely experiences more frequent changes in water table levels compared to the Ward peat bog. This likely imparts a higher degree of tolerance for hydrological and O_2 variability in the PB peat. These results are comparable to the observations in (46), where dry-wet manipulations in a Boreal minerotrophic fen did not stimulate phenol oxidase activity or enhance CH_4 production, despite an initial surge in CO_2 production. They also observed an increase in sulfate, Fe(III), and nitrate concentrations upon soil drying. While nitrate levels in the PB peat was below detection limit throughout, the increase in sulfate concentrations we observed (~112 uM) were largely comparable to those reported in (46) (>100 uM). At least part of

the carbon flow in PB peat may have thus been directed towards anaerobic respiration, specifically sulfate reduction, which is further supported by the relatively higher expression of Dsr genes and putative sulfate reducers in the PB peat metatranscriptomes (Fig. 3b,c). These results also compare to the recent observation that carbon decomposition in Northern peatlands is likely dominated by TEA respiration rather than methanogenesis (49). Geochemical and microbial data thus indicate that unlike in Ward peat, phenolic compounds may not comprise a strong "latch" on PB peat carbon degradation. In agreement with field-based studies (46), our observations collectively suggest that O_2 fluctuations in minerotrophic fen systems likely will not lead to stimulated CH_4 emissions.

Additionally, the strikingly dissimilar response of the saltmarsh sediments to transient oxygenation points to varying microbial community compositions and ionic interactions shaped by salinity and sulfate levels, which may cause divergent responses of brackish coastal wetlands to O_2 shifts. Systems subjected to tidal flushing and associated periodic changes in O_2 levels may, however, be more buffered against O_2 variability.

Wetland resiliency to O_2 *shifts in the context of global change.*

Our observations indicate divergent levels of resiliency of wetland systems to O_2 shifts, with important implications for wetland management under climate change scenarios. Compared to bogs, mineral soil wetlands such as the FW marsh, and minerotrophic peatlands supporting alternative respiration, such as PB peat, are more resilient to O_2 shifts. Partly, this resilience could stem from "memory effects" due to frequent redox changes that could confer microbial communities with the capacity to adapt. Such resiliency may be absent in permanently anoxic sediments of saltmarshes as we observed a clear lack of convergence between the O_2-shifted and anoxic saltmarsh samples. While the validity of these results to field settings remains to be assessed, our observations indicate potentially major, persistent changes in saltmarsh ecosystems as a result of redox variability that could result from coastal restoration or sea-level rise. The large heterogeneity in the susceptibility of wetland carbon stock to oxygen variability (or dry-wet cycles) is well-documented (reviewed in (87)), yet the pertinent mechanisms remain unknown. Our observations point out specific microbial taxa as potential indicators of wetland resiliency under hydrological variations, and indicate the microbiome data can inform predictions of wetland biogeochemical behavior upon redox shifts. These results also underscore the need to assess wetland resiliency in the context of their divergent ecological settings. Such careful characterization of the environmental heterogeneity is essential for accurately scaling up laboratory observations to predictive global models of peatland methane emission trajectories.

DATA AVAILABILITY STATEMENT

All sequence data has been deposited in the NCBI Sequence Read Archive under the BioProject accession PRJNA1123272 (data will be publicly available upon publication). All other datasets and R codes used for analyses and for generating the figures are available at the GitHub repository (https://github.com/Linta-Reji/Reji2024_wetland_O2shifts), with large files uploaded to Zenodo (doi: 10.5281/zenodo.14510955).

CONFLICT OF INTERESTS

The authors declare no competing interests.

ACKNOWLEDGMENTS

This study was supported by the Carbon Mitigation Initiative at the High Meadows Environmental Research Institute at Princeton University. The authors thank Dr. E. Han for assistance with sample collection. The authors are pleased to acknowledge that the work reported on in this paper was substantially performed using the Princeton Research Computing resources at Princeton University which is consortium of groups led by the Princeton Institute for Computational Science and Engineering (PICSciE) and Office of Information Technology's Research Computing. This work was supported by the Office of Science, Office of Biological and Environmental Research, of the US Department of Energy under Award Numbers DE-AC02-05CH11231, DE-AC02-06CH11357, DE-AC05-00OR22725, and DE-AC02-98CH10886, as part of the DOE Systems Biology Knowledgebase.

References

1. Lal R. Carbon sequestration. Philos Trans R Soc B Biol Sci. 2007 Aug 30;363(1492):815–30.

2. Mitsch WJ, Bernal B, Nahlik AM, Mander Ü, Zhang L, Anderson CJ, et al. Wetlands, carbon, and climate change. Landsc Ecol. 2013 Apr 1;28(4):583–97.

3. McLatchey GP, Reddy KR. Regulation of Organic Matter Decomposition and Nutrient Release in a Wetland Soil. J Environ Qual. 1998;27(5):1268–74.

4. Limpens J, Berendse F, Blodau C, Canadell JG, Freeman C, Holden J, et al. Peatlands and the carbon cycle: from local processes to global implications – a synthesis. Biogeosciences. 2008 Oct 31;5(5):1475–91.

5. Zhao J, Malone SL, Oberbauer SF, Olivas PC, Schedlbauer JL, Staudhammer CL, et al. Intensified inundation shifts a freshwater wetland from a CO2 sink to a source. Glob Change Biol. 2019;25(10):3319–33.

6. Anderson B, Bartlett K, Frolking S, Hayhoe K, Jenkins J, Salas W. Methane and Nitrous Oxide Emissions from Natural Sources. Earth Sci [Internet]. 2010 Apr 1; Available from: https://scholars.unh.edu/earthsci_facpub/484

7. Tian H, Chen G, Lu C, Xu X, Ren W, Zhang B, et al. Global methane and nitrous oxide emissions from terrestrial ecosystems due to multiple environmental changes. Ecosyst Health Sustain. 2015;1(1):1–20.

8. Zou J, Ziegler AD, Chen D, McNicol G, Ciais P, Jiang X, et al. Rewetting global wetlands effectively reduces major greenhouse gas emissions. Nat Geosci. 2022 Aug;15(8):627–32.

9. Saunois M, Martinez A, Poulter B, Zhang Z, Raymond P, Regnier P, et al. Global Methane Budget 2000–2020 [Internet]. 2024 [cited 2024 Nov 7]. Available from: https://essd.copernicus.org/preprints/essd-2024-115/

10. Koffi EN, Bergamaschi P, Alkama R, Cescatti A. An observation-constrained assessment of the climate sensitivity and future trajectories of wetland methane emissions. Sci Adv. 2020 Apr;6(15):eaay4444.

11. Zhang Z, Zimmermann NE, Stenke A, Li X, Hodson EL, Zhu G, et al. Emerging role of wetland methane emissions in driving 21st century climate change. Proc Natl Acad Sci U S A. 2017 Sep 5;114(36):9647–52.

12. Saunois M, Stavert AR, Poulter B, Bousquet P, Canadell JG, Jackson RB, et al. The Global Methane Budget 2000–2017. Earth Syst Sci Data. 2020 Jul 15;12(3):1561–623.

13. Fenner N, Freeman C. Drought-induced carbon loss in peatlands. Nat Geosci. 2011 Dec;4(12):895–900.

14. Malone SL, Starr G, Staudhammer CL, Ryan MG. Effects of simulated drought on the carbon balance of Everglades short-hydroperiod marsh. Glob Change Biol. 2013;19(8):2511–23.

15. Li J, Jiang M, Pei J, Fang C, Li B, Nie M. Convergence of carbon sink magnitude and water table depth in global wetlands. Ecol Lett. 2023;26(5):797–804.

16. Zhu J, Sun G, Li W, Zhang Y, Miao G, Noormets A, et al. Modeling the potential impacts of climate change on the water table level of selected forested wetlands in the southeastern United States. Hydrol Earth Syst Sci. 2017 Dec 13;21(12):6289–305.

17. Ma L, Zhu G, Chen B, Zhang K, Niu S, Wang J, et al. A globally robust relationship between water table decline, subsidence rate, and carbon release from peatlands. Commun Earth Environ. 2022 Oct 29;3(1):1–14.

18. Megonigal JP, Hines ME, Visscher PT. 8.08 - Anaerobic Metabolism: Linkages to Trace Gases and Aerobic Processes. In: Holland HD, Turekian KK, editors. Treatise on Geochemistry [Internet]. Oxford: Pergamon; 2003 [cited 2024 May 28]. p. 317–424. Available from: https://www.sciencedirect.com/science/article/pii/B0080437516081329

19. Updegraff K, Bridgham SD, Pastor J, Weishampel P, Harth C. Response of Co2 and Ch4 Emissions from Peatlands to Warming and Water Table Manipulation. Ecol Appl. 2001;11(2):311–26.

20. Goodrich JP, Campbell DI, Roulet NT, Clearwater MJ, Schipper LA. Overriding control of methane flux temporal variability by water table dynamics in a Southern Hemisphere, raised bog. J Geophys Res Biogeosciences. 2015;120(5):819–31.

21. Teh YA, Silver WL, Conrad ME. Oxygen effects on methane production and oxidation in humid tropical forest soils. Glob Change Biol. 2005 Aug;11(8):1283–97.

22. Angel R, Matthies D, Conrad R. Activation of Methanogenesis in Arid Biological Soil Crusts Despite the Presence of Oxygen. PLOS ONE. 2011 May 31;6(5):e20453.

23. Angle JC, Morin TH, Solden LM, Narrowe AB, Smith GJ, Borton MA, et al. Methanogenesis in oxygenated soils is a substantial fraction of wetland methane emissions. Nat Commun. 2017 Nov 16;8(1):1567.

24. Yang WH, McNicol G, Teh YA, Estera-Molina K, Wood TE, Silver WL. Evaluating the Classical Versus an Emerging Conceptual Model of Peatland Methane Dynamics. Glob Biogeochem Cycles. 2017;31(9):1435–53.

25. Wilmoth JL, Schaefer JK, Schlesinger DR, Roth SW, Hatcher PG, Shoemaker JK, et al. The role of oxygen in stimulating methane production in wetlands. Glob Change Biol. 2021 Nov;27(22):5831–47.

26. Freeman C, Ostle NJ, Fenner N, Kang H. A regulatory role for phenol oxidase during decomposition in peatlands. Soil Biol Biochem. 2004 Oct 1;36(10):1663–7.

27. Freeman C, Ostle N, Kang H. An enzymic "latch" on a global carbon store. Nature. 2001 Jan 11;409(6817):149.

28. Fenner N, Freeman C. Woody litter protects peat carbon stocks during drought. Nat Clim Change. 2020 Apr;10(4):363–9.

29. Reji L, Zhang X. Genome-Resolved Metagenomics Informs the Functional Ecology of Uncultured Acidobacteria in Redox Oscillated Sphagnum Peat. mSystems. 7(5):e00055-22.

30. Reddy KR, DeLaune RD, Inglett PW. Biogeochemistry of Wetlands: Science and Applications. 2nd ed. Boca Raton: CRC Press; 2022. 732 p.

31. Arnold W, Taylor M, Bradford M, Raymond P, Peccia J. Microbial activity contributes to spatial heterogeneity of wetland methane fluxes. Microbiol Spectr. 2023 Sep 20;11(5):e02714-23.

32. Cui S, Liu P, Guo H, Nielsen CK, Pullens JWM, Chen Q, et al. Wetland hydrological dynamics and methane emissions. Commun Earth Environ. 2024 Aug 29;5(1):1–17.

33. Brouns K, Verhoeven JTA, Hefting MM. Short period of oxygenation releases latch on peat decomposition. Sci Total Environ. 2014 May 15;481:61–8.

34. Hall SJ, Treffkorn J, Silver WL. Breaking the enzymatic latch: impacts of reducing conditions on hydrolytic enzyme activity in tropical forest soils. Ecology. 2014;95(10):2964–73.

35. Romanowicz KJ, Kane ES, Potvin LR, Daniels AL, Kolka RK, Lilleskov EA. Understanding drivers of peatland extracellular enzyme activity in the PEATcosm experiment: mixed evidence for enzymic latch hypothesis. Plant Soil. 2015 Dec 1;397(1):371–86.

36. McGivern BB, Tfaily MM, Borton MA, Kosina SM, Daly RA, Nicora CD, et al. Decrypting bacterial polyphenol metabolism in an anoxic wetland soil. Nat Commun. 2021 Apr 29;12(1):2466.

37. Lankiewicz TS, Choudhary H, Gao Y, Amer B, Lillington SP, Leggieri PA, et al. Lignin deconstruction by anaerobic fungi. Nat Microbiol. 2023 Apr;8(4):596–610.

38. McGivern BB, Cronin DR, Ellenbogen JB, Borton MA, Knutson EL, Freire-Zapata V, et al. Microbial polyphenol metabolism is part of the thawing permafrost carbon cycle. Nat Microbiol. 2024 Jun;9(6):1454–66.

39. Van Bodegom PM, Broekman R, Van Dijk J, Bakker C, Aerts R. Ferrous Iron Stimulates Phenol Oxidase Activity and Organic Matter Decomposition in Waterlogged Wetlands. Biogeochemistry. 2005;76(1):69–83.

40. Hall SJ, Silver WL. Iron oxidation stimulates organic matter decomposition in humid tropical forest soils. Glob Change Biol. 2013;19(9):2804–13.

41. Wang Y, Wang H, He JS, Feng X. Iron-mediated soil carbon response to water-table decline in an alpine wetland. Nat Commun. 2017 Jun 26;8(1):15972.

42. Wen Y, Zang H, Ma Q, Evans CD, Chadwick DR, Jones DL. Is the 'enzyme latch' or 'iron gate' the key to protecting soil organic carbon in peatlands? Geoderma. 2019 Sep 1;349:107–13.

43. Dong H, Zeng Q, Sheng Y, Chen C, Yu G, Kappler A. Coupled iron cycling and organic matter transformation across redox interfaces. Nat Rev Earth Environ. 2023 Sep;4(9):659–73.

44. Li B, Rodell M. How Have Hydrological Extremes Changed over the Past 20 Years? J Clim. 2023 Nov 28;36(24):8581–99.

45. Rodell M, Li B. Changing intensity of hydroclimatic extreme events revealed by GRACE and GRACE-FO. Nat Water. 2023 Mar;1(3):241–8.

46. Reiche M, Hädrich A, Lischeid G, Küsel K. Impact of manipulated drought and heavy rainfall events on peat mineralization processes and source-sink functions of an acidic fen. J Geophys Res Biogeosciences [Internet]. 2009 [cited 2024 May 29];114(G2). Available from: https://onlinelibrary.wiley.com/doi/abs/10.1029/2008JG000853

47. Bridgham SD, Cadillo-Quiroz H, Keller JK, Zhuang Q. Methane emissions from wetlands: biogeochemical, microbial, and modeling perspectives from local to global scales. Glob Change Biol. 2013 May;19(5):1325–46.

48. Song T, Liu Y, Kolton M, Wilson RM, Keller JK, Rolando JL, et al. Porewater constituents inhibit microbially mediated greenhouse gas production (GHG) and regulate the response of soil organic matter decomposition to warming in anoxic peat from a Sphagnum-dominated bog. FEMS Microbiol Ecol. 2023 Jul 1;99(7):fiad060.

49. Duchesneau K, Riquelme BA, Petro C, Makke G, Green M, Tfaily M, et al. Northern peatland microbial networks exhibit resilience to warming and acquire electron acceptor from soil organic matter [Internet]. bioRxiv; 2024 [cited 2024 Dec 17]. p. 2024.07.17.603906. Available from: https://www.biorxiv.org/content/10.1101/2024.07.17.603906v1

50. Hanson BA. ChemoSpec: Exploratory Chemometrics for Spectroscopy [Internet]. 2024. Available from: https://bryanhanson.github.io/ChemoSpec/.

51. R Core Team. R Foundation for Statistical Computing, Vienna, Austria. [cited 2024 May 30]. R: A language and environment for statistical computing. Available from: https://www.r-project.org/

52. Wickham H, Averick M, Bryan J, Chang W, McGowan LD, François R, et al. Welcome to the Tidyverse. J Open Source Softw. 2019 Nov 21;4(43):1686.

53. Martin M. Cutadapt removes adapter sequences from high-throughput sequencing reads. EMBnet.journal. 2011 May 2;17(1):10–2.

54. Callahan BJ, McMurdie PJ, Rosen MJ, Han AW, Johnson AJA, Holmes SP. DADA2: High-resolution sample inference from Illumina amplicon data. Nat Methods. 2016 Jul;13(7):581–3.

55. Quast C, Pruesse E, Yilmaz P, Gerken J, Schweer T, Yarza P, et al. The SILVA ribosomal RNA gene database project: improved data processing and web-based tools. Nucleic Acids Res. 2013 Jan;41(Database issue):D590–6.

56. McMurdie PJ, Holmes S. phyloseq: An R Package for Reproducible Interactive Analysis and Graphics of Microbiome Census Data. PLOS ONE. 2013 Apr 22;8(4):e61217.

57. Barnett DJ m, Arts IC w, Penders J. microViz: an R package for microbiome data visualization and statistics. J Open Source Softw. 2021 Jul 10;6(63):3201.

58. Dahl EM, Neer E, Bowie KR, Leung ET, Karstens L. microshades: An R Package for Improving Color Accessibility and Organization of Microbiome Data. Microbiol Resour Announc. 2022 Oct 31;11(11):e00795-22.

59. Mandal S, Van Treuren W, White RA, Eggesbø M, Knight R, Peddada SD. Analysis of composition of microbiomes: a novel method for studying microbial composition. Microb Ecol Health Dis. 2015 Dec 1;26(1):27663.

60. Lin H, Peddada SD. Analysis of compositions of microbiomes with bias correction. Nat Commun. 2020 Jul 14;11(1):3514.

61. Andrews S. FastQC: A Quality Control tool for High Throughput Sequence Data [Internet]. [cited 2024 May 30]. Available from: https://www.bioinformatics.babraham.ac.uk/projects/fastqc/

62. Bolger AM, Lohse M, Usadel B. Trimmomatic: a flexible trimmer for Illumina sequence data. Bioinformatics. 2014 Aug 1;30(15):2114–20.

63. Eren AM, Kiefl E, Shaiber A, Veseli I, Miller SE, Schechter MS, et al. Community-led, integrated, reproducible multi-omics with anvi'o. Nat Microbiol. 2021 Jan;6(1):3–6.

64. Li D, Liu CM, Luo R, Sadakane K, Lam TW. MEGAHIT: an ultra-fast single-node solution for large and complex metagenomics assembly via succinct de Bruijn graph. Bioinforma Oxf Engl. 2015 May 15;31(10):1674–6.

65. Li D, Luo R, Liu CM, Leung CM, Ting HF, Sadakane K, et al. MEGAHIT v1.0: A fast and scalable metagenome assembler driven by advanced methodologies and community practices. Methods San Diego Calif. 2016 Jun 1;102:3–11.

66. Langmead B, Salzberg SL. Fast gapped-read alignment with Bowtie 2. Nat Methods. 2012 Apr;9(4):357–9.

67. Kang DD, Li F, Kirton E, Thomas A, Egan R, An H, et al. MetaBAT 2: an adaptive binning algorithm for robust and efficient genome reconstruction from metagenome assemblies. PeerJ. 2019 Jul 26;7:e7359.

68. Wu YW, Simmons BA, Singer SW. MaxBin 2.0: an automated binning algorithm to recover genomes from multiple metagenomic datasets. Bioinformatics. 2016 Feb 1;32(4):605–7.

69. Alneberg J, Bjarnason BS, de Bruijn I, Schirmer M, Quick J, Ijaz UZ, et al. Binning metagenomic contigs by coverage and composition. Nat Methods. 2014 Nov;11(11):1144–6.

70. Uritskiy GV, DiRuggiero J, Taylor J. MetaWRAP—a flexible pipeline for genome-resolved metagenomic data analysis. Microbiome. 2018 Sep 15;6(1):158.

71. Hyatt D, Chen GL, LoCascio PF, Land ML, Larimer FW, Hauser LJ. Prodigal: prokaryotic gene recognition and translation initiation site identification. BMC Bioinformatics. 2010 Mar 8;11(1):119.

72. Kanehisa M, Sato Y, Morishima K. BlastKOALA and GhostKOALA: KEGG Tools for Functional Characterization of Genome and Metagenome Sequences. J Mol Biol. 2016 Feb 22;428(4):726–31.

73. Shaffer M, Borton MA, McGivern BB, Zayed AA, La Rosa SL, Solden LM, et al. DRAM for distilling microbial metabolism to automate the curation of microbiome function. Nucleic Acids Res. 2020 Sep 18;48(16):8883–900.

74. Brettin T, Davis JJ, Disz T, Edwards RA, Gerdes S, Olsen GJ, et al. RASTtk: A modular and extensible implementation of the RAST algorithm for building custom annotation pipelines and annotating batches of genomes. Sci Rep. 2015 Feb 10;5(1):8365.

75. Arkin AP, Cottingham RW, Henry CS, Harris NL, Stevens RL, Maslov S, et al. KBase: The United States Department of Energy Systems Biology Knowledgebase. Nat Biotechnol. 2018 Aug;36(7):566–9.

76. Hodgkins SB, Tfaily MM, Podgorski DC, McCalley CK, Saleska SR, Crill PM, et al. Elemental composition and optical properties reveal changes in dissolved organic matter along a permafrost thaw chronosequence in a subarctic peatland. Geochim Cosmochim Acta. 2016 Aug 15;187:123–40.

77. McGivern BB, Tfaily MM, Borton MA, Kosina SM, Daly RA, Nicora CD, et al. Decrypting bacterial polyphenol metabolism in an anoxic wetland soil. Nat Commun. 2021 Apr 29;12(1):2466.

78. Urbanová Z, Hájek T. Revisiting the concept of 'enzymic latch' on carbon in peatlands. Sci Total Environ. 2021 Jul 20;779:146384.

79. Hájek T, Ballance S, Limpens J, Zijlstra M, Verhoeven JTA. Cell-wall polysaccharides play an important role in decay resistance of Sphagnum and actively depressed decomposition in vitro. Biogeochemistry. 2011 Apr 1;103(1):45–57.

80. Pipes GT, Yavitt JB. Biochemical components of Sphagnum and persistence in peat soil. Can J Soil Sci. 2022 Apr;102(3):785–95.

81. Zhao Y, Liu C, Li X, Ma L, Zhai G, Feng X. Sphagnum increases soil's sequestration capacity of mineral-associated organic carbon via activating metal oxides. Nat Commun. 2023 Aug 19;14(1):5052.

82. Wilson RM, Tfaily MM, Rich VI, Keller JK, Bridgham SD, Zalman CM, et al. Hydrogenation of organic matter as a terminal electron sink sustains high CO2:CH4 production ratios during anaerobic decomposition. Org Geochem. 2017 Oct 1;112:22–32.

83. Spratt HG, Morgan MD, Good RE. Sulfate reduction in peat from a new jersey pinelands cedar swamp. Appl Environ Microbiol. 1987 Jul;53(7):1406–11.

84. Gardner W, Lee GF. Oxygenation of Lake Sediments. Int J Air Water Pollut. 1965;9:553–64.

85. Rickard D, Luther GW. Chemistry of Iron Sulfides. Chem Rev. 2007 Feb 1;107(2):514–62.

86. Ingvorsen K, Zehnder AJB, Jørgensen BB. Kinetics of Sulfate and Acetate Uptake by Desulfobacter postgatei. Appl Environ Microbiol. 1984 Feb;47(2):403–8.

87. Laiho R. Decomposition in peatlands: Reconciling seemingly contrasting results on the impacts of lowered water levels. Soil Biol Biochem. 2006 Aug 1;38(8):2011–24.

Figures

Figure 1:

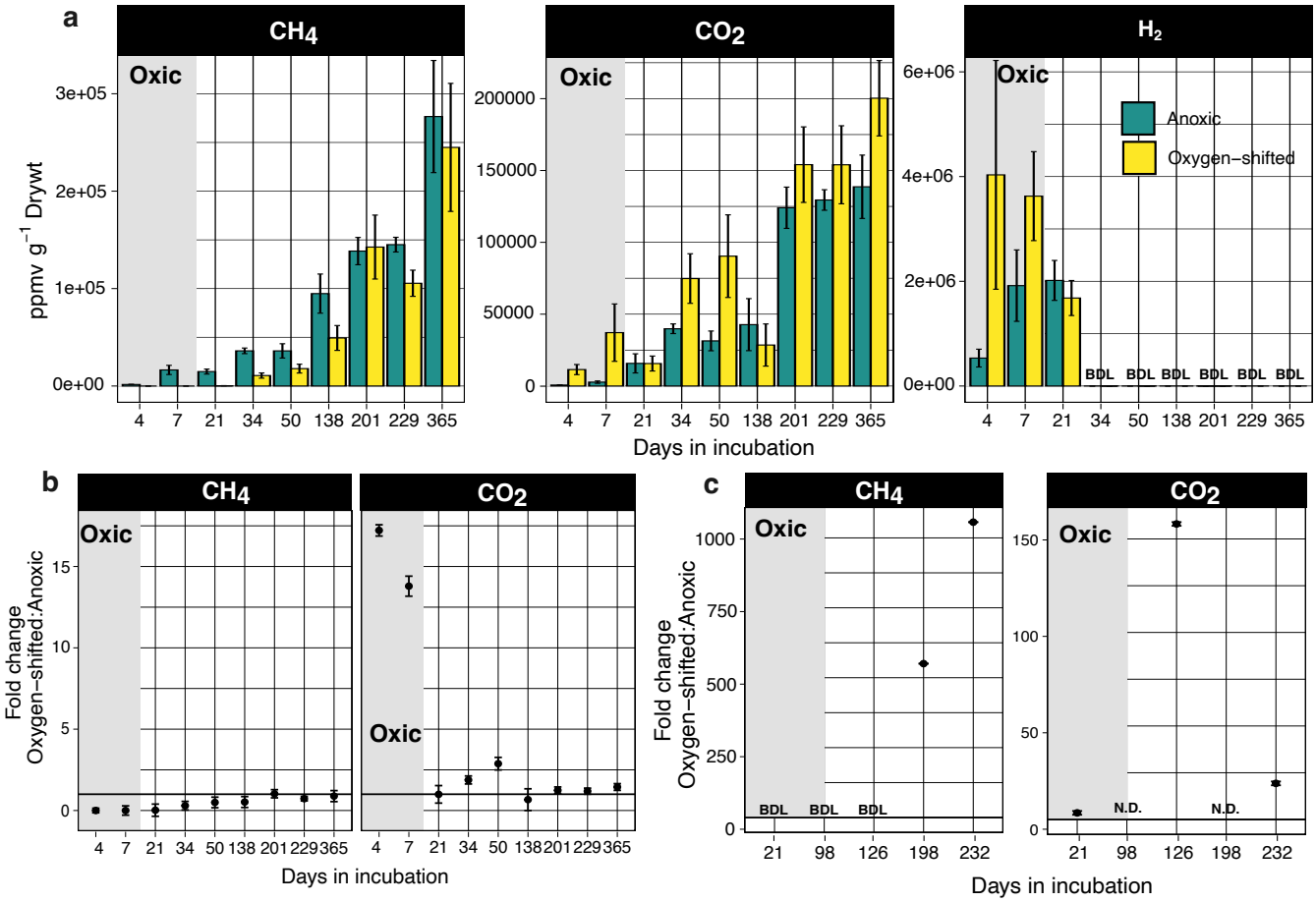

Figure 1: Trace gases measured in the fen-origin PB peat incubation headspaces (a,b) and compared to those in bog-origin Ward peat (c). (a) For PB peat, concentrations of CH_4, CO_2, and H_2 across incubation time points. The grey rectangle indicates the oxic period for the O_2-shifted samples. Error bars are standard errors around the mean of three replicates. (**b**) For PB peat, fold change in headspace CH_4 and CO_2 concentrations between the O_2-shifted and continuously anoxic incubations. A fold change of 1 indicates no difference between the two treatments. (c) For Ward peat, fold change in CH_4 and CO_2 concentrations between O_2-shifted and continuously anoxic incubations. Data replotted from ref. 24. Oxic period is indicated by the grey rectangle in each plot. N.D., not determined. BDL: below detection limit.

Figure 2:

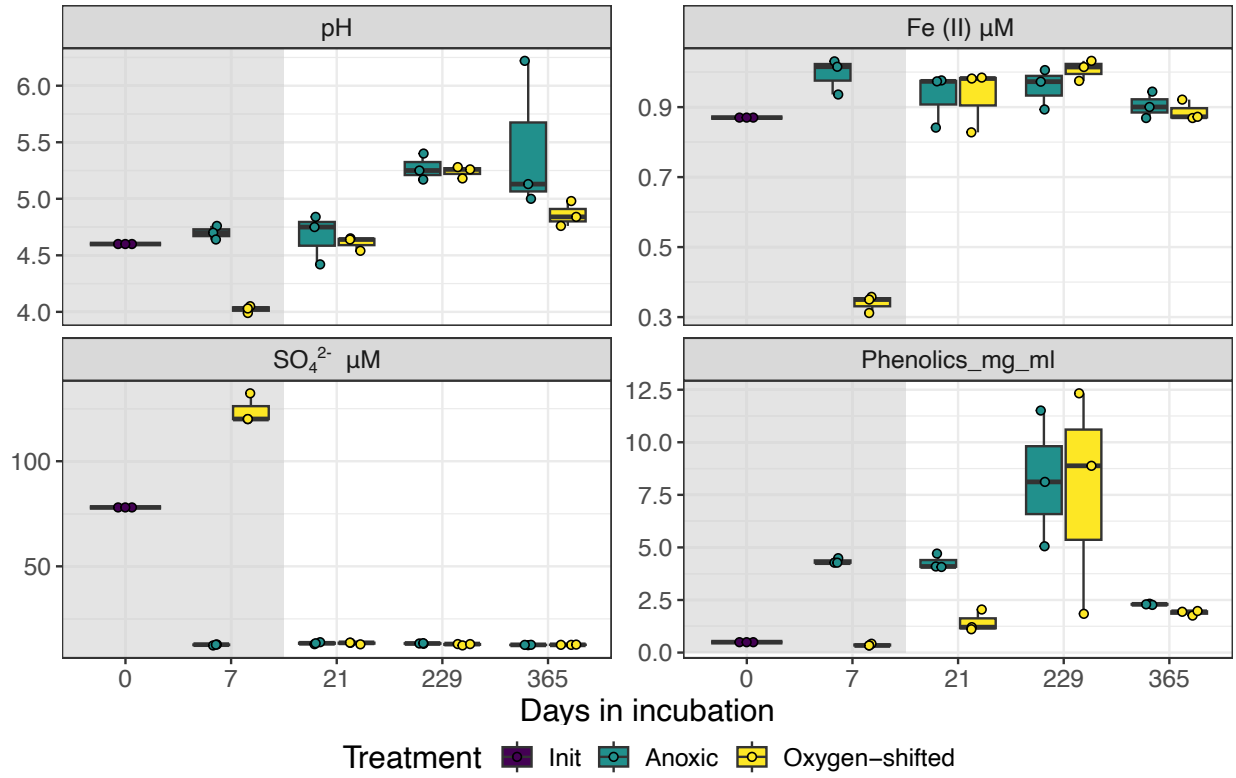

Figure 2: Changes in wetland soil geochemistry with the O_2 shift. Key geochemical variables measured in PB peat across timepoints in the experiment. Oxic period is indicated by the grey rectangle. Three replicate measurements are included in each boxplot (overlayed dots depict the actual values). N.D., not determined. Phenolics concentrations were measured as mg/ml gallic acid-equivalent.

Figure 3:

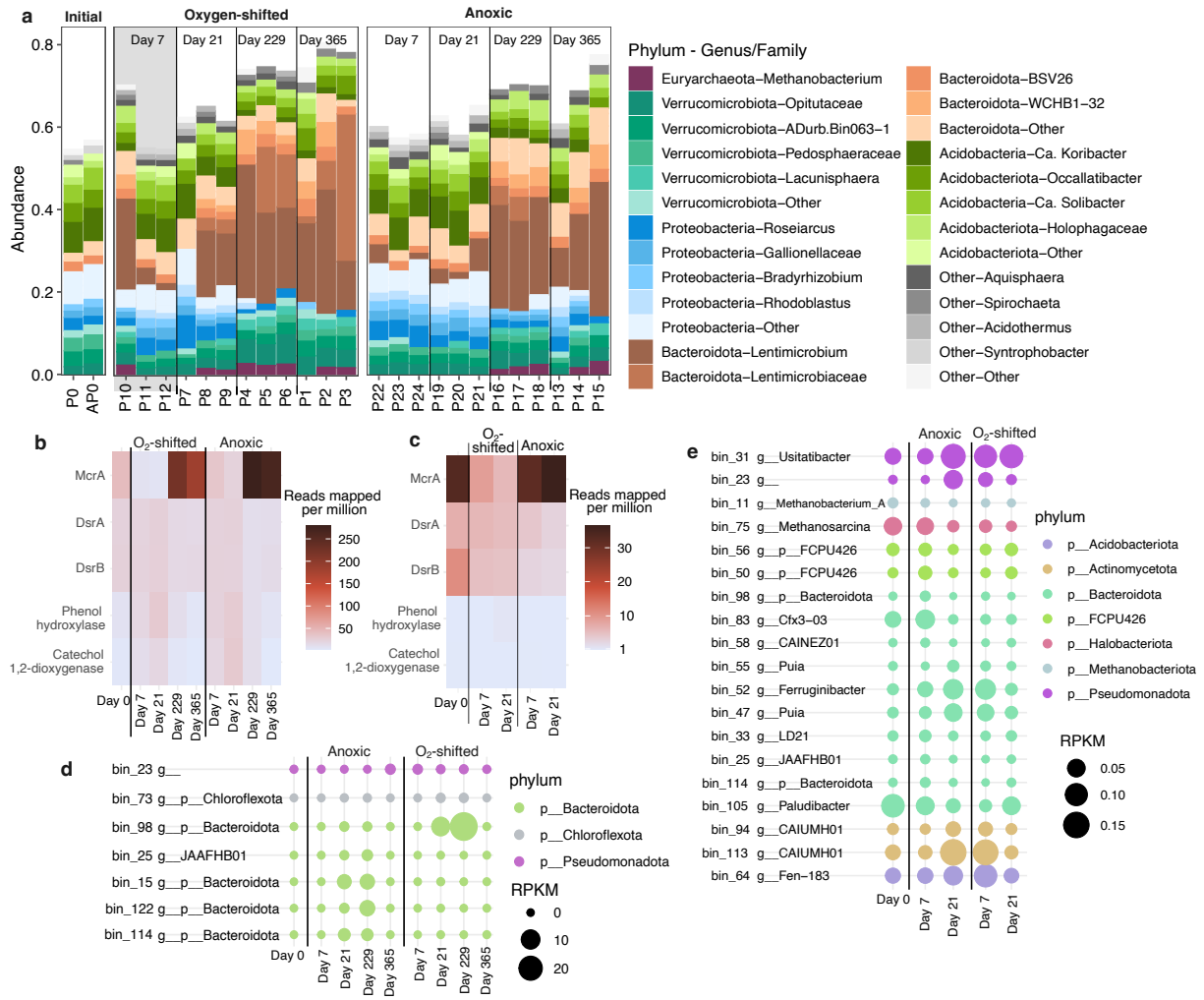

Figure 3: PB peat microbial community response to the O_2 shift. Microbial community composition across incubation timepoints assessed using the V4 region of 16S rRNA gene. (**a**) Top 5 phyla comprising >50% of the community in the PB peat microbiome. Dominant genus or family-level lineages are also highlighted for each phylum. Gray box in the "Oxygen-shifted" panel indicates replicate samples at the end of the oxic period. (b) Relative abundances of selected functions in the PB peat metagenomes. McrA: methyl coenzyme reductase; DsrA and DsrB: sulfite reductase subunits A and B. (**c**) Relative abundance of the selected functions in the PB peat metatranscriptomes. MAGs identified as differentially abundant (d) and active (c) between O_2 treatments in PB peat. For each MAG, taxonomic identity at the genus, family, or phylum-level has been presented. RPKM: reads mapped per kilobase of genomes per million total reads.

Figure 4:

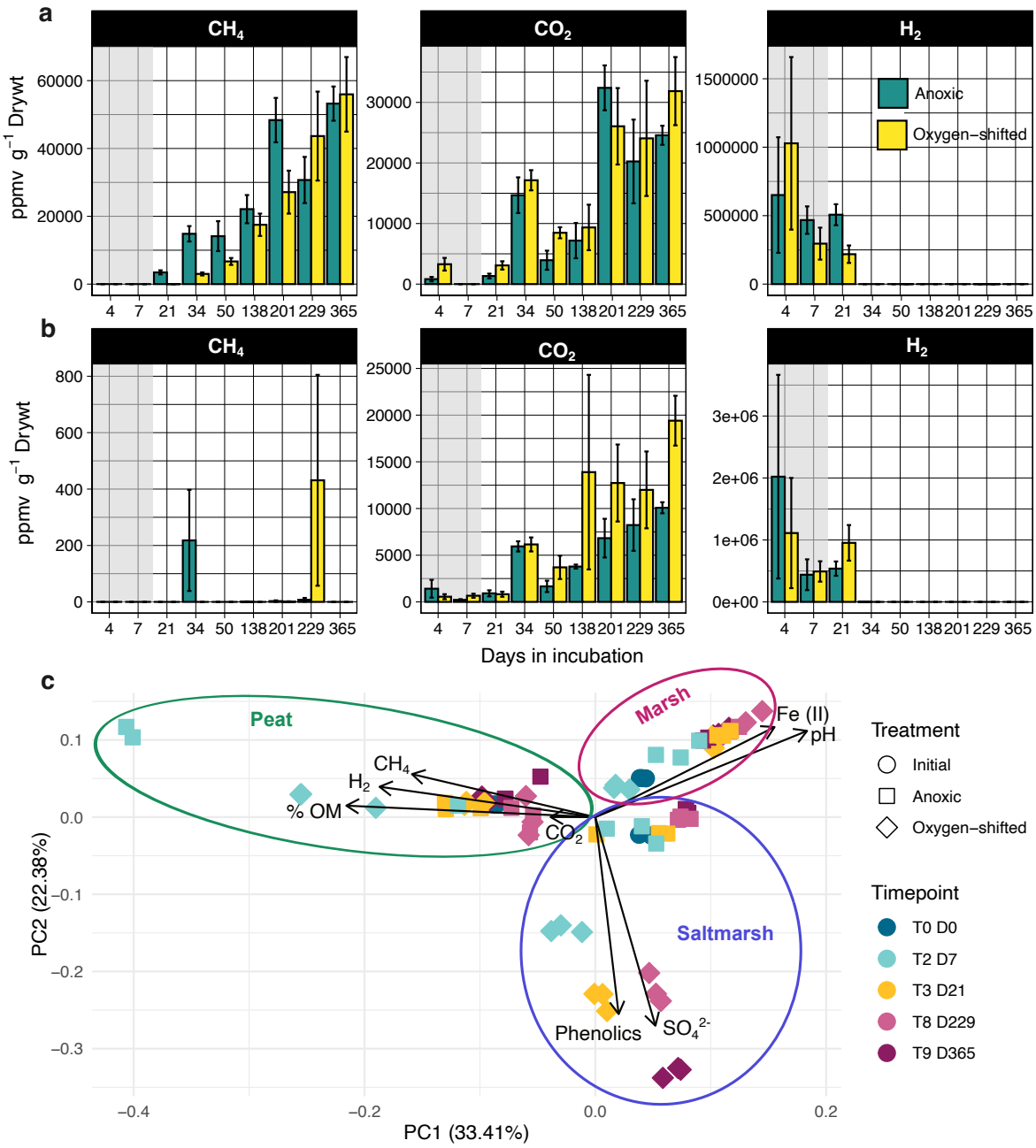

Figure 4: Geochemical responses of FW-marsh and saltmarsh to O_2 shift. CH_4, CO_2, and H_2 measured in the incubation headspaces across timepoints in FW marsh (**a**) and saltmarsh (**b**). The grey rectangle indicates the oxic period for the O_2-shifted samples. Error bars are standard errors around the mean of three replicates. (**c**) PCA of key geochemical variables measured over the course of the experiment. Shapes indicate different treatments. Ellipses are drawn to indicate each wetland type.

Figure 5:

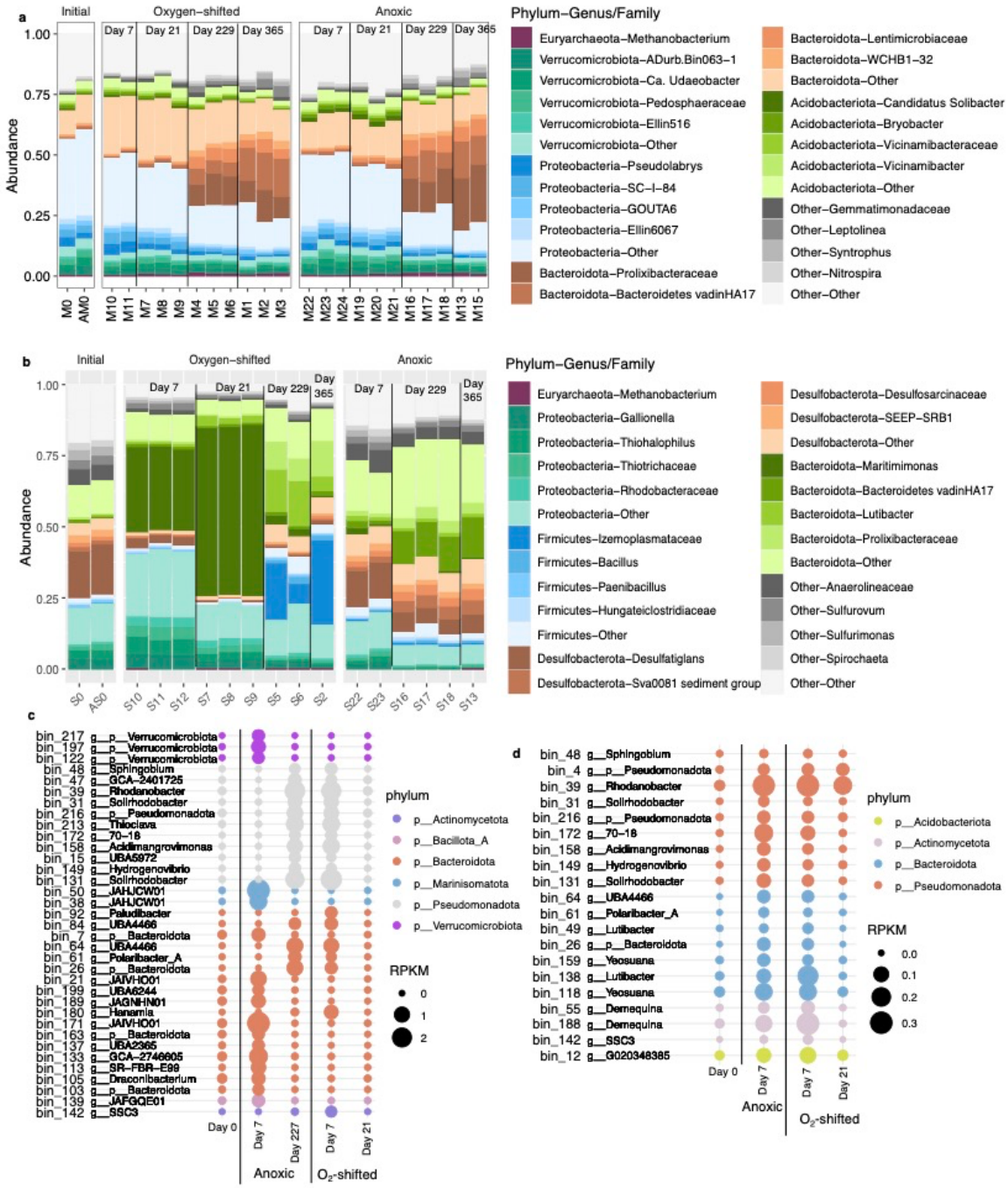

Figure 5: Microbiome response to O2 shift in FW-marsh and saltmarsh. Microbial community composition across time points in FW-marsh (a) and saltmarsh (b), assessed using the V4 region of 16S rRNA gene. Top 5 phyla comprising >50% of the communities are highlighted in each plot. Dominant genus or family-level lineages are also indicated for each phylum. (b) MAGs identified as differentially abundant (d) and active (c) between O_2 treatments in the saltmarsh incubations. For each MAG, taxonomic identity at the genus, family, or phylum-level has been presented. RPKM: reads mapped per kilobase of genomes per million total reads.

Figure 6: Schematic diagram of microbially-mediated carbon flow with O_2 shift in the (a) Ward sphagnum peat compared to (b) PB Sphagnum peat. In contrast to Ward peat, transient oxygenation does not lead to a surge in anoxic CH_4 production in PB peat, likely due to (i) the PB fen being subject to fluctuations in water (and thus oxygen) levels, favoring a microbiome with lower sensitivity to O_2 variability, and (ii) alternative terminal electron acceptors redirecting carbon flow away from CH_4. The width of the arrows presents the importance of relevant metabolisms.

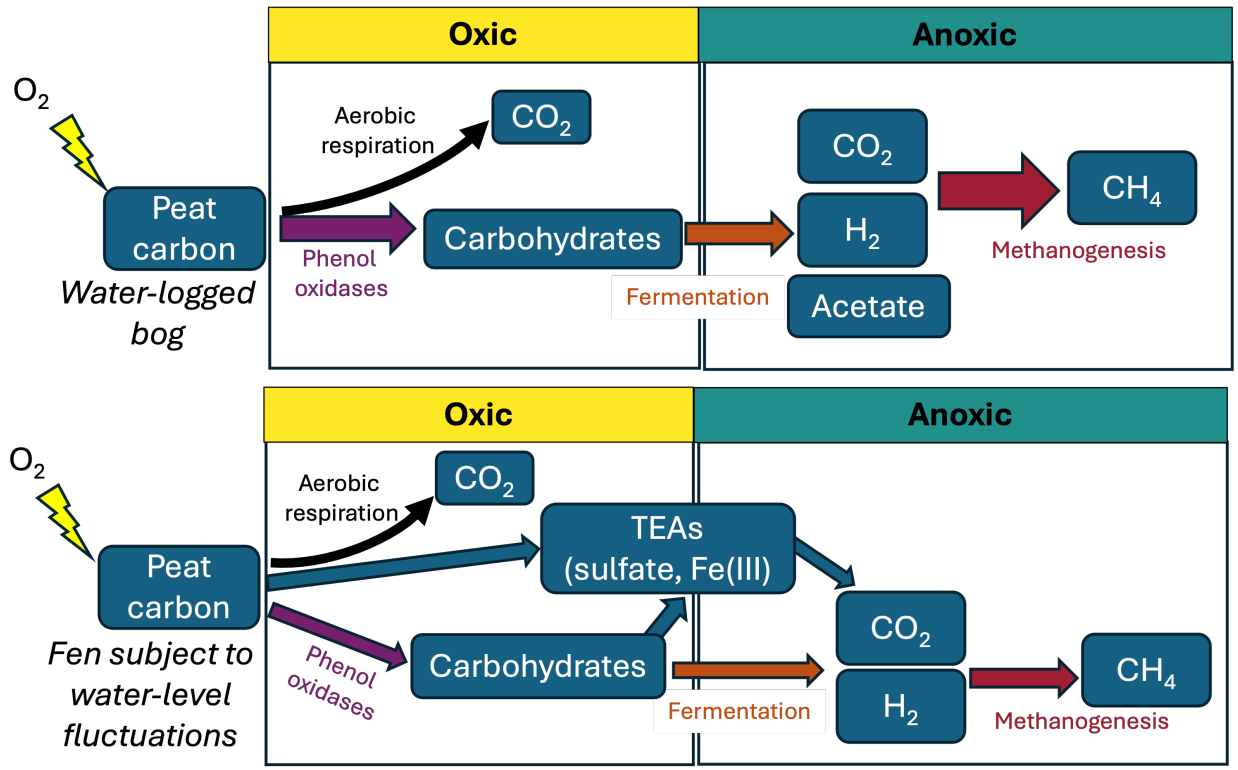

Supplementary Figures

Figure S1:

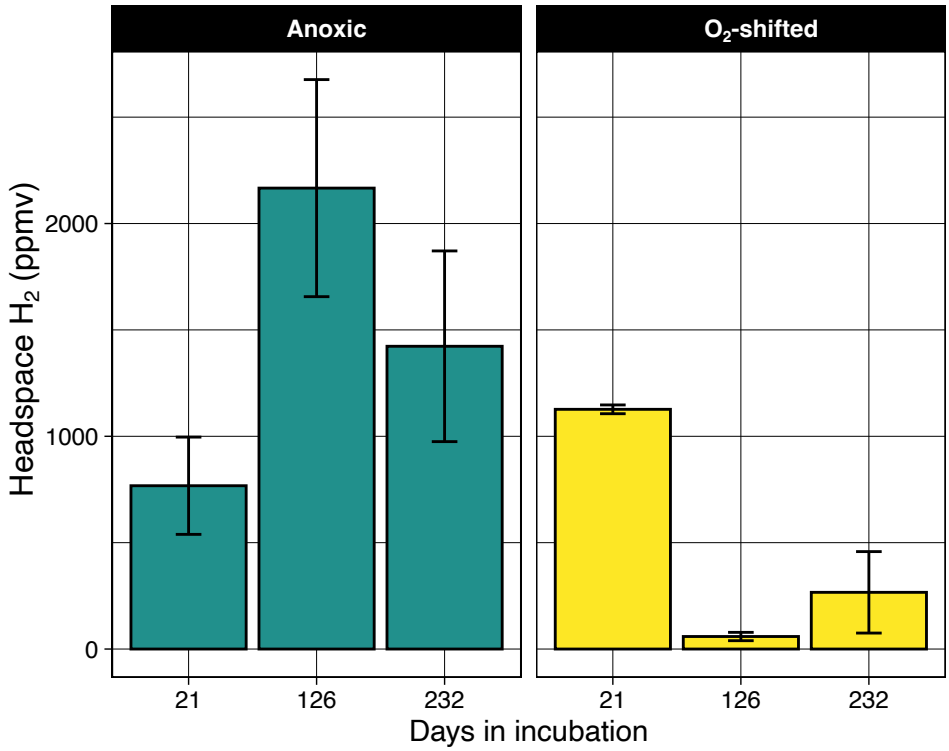

Figure S1: H_2 Measured in Ward peat incubations. Error bars are standard errors around the mean of three replicates. Data re-plotted from (24).

Figure S2:

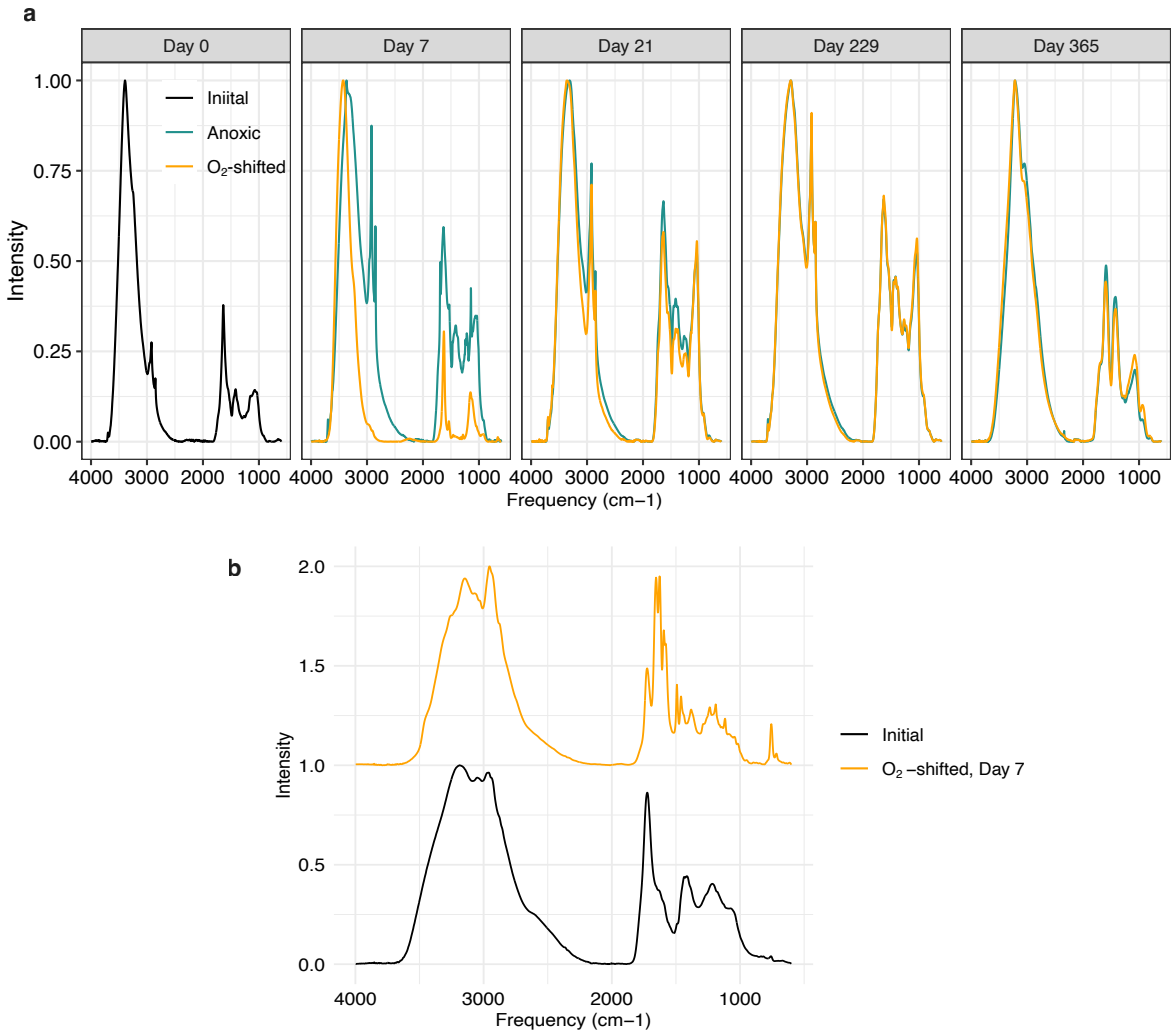

Figure S2: FTIR spectra of PB peat slurry extracts (**a**) and after desalting for the Day 7 samples (**b**). The Day 7 samples were desalted and compared due to significant salt interferences (indicated by the strong O–H bending band at 1620 cm^{-1}) in the O_2-shifted sample (**a**).

Figure S3:

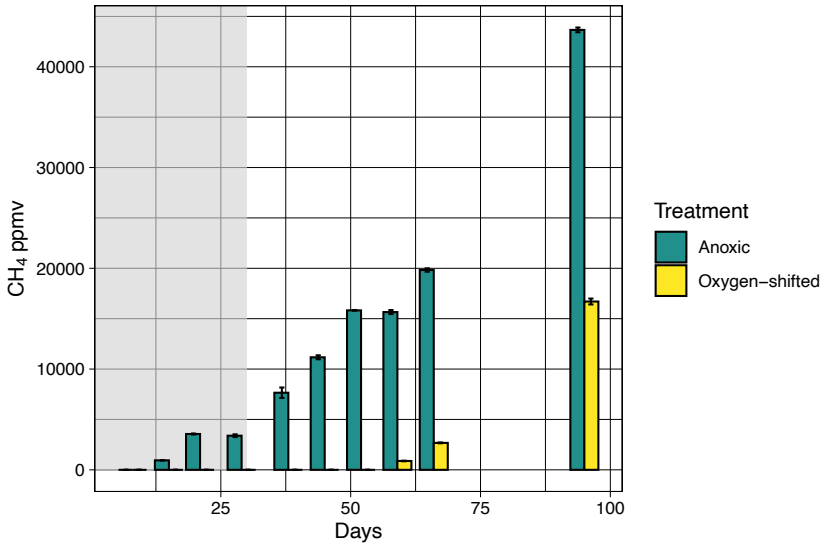

Figure S3: Headspace methane concentrations in the PB peat incubations when PB peat was exposed to a longer period of oxygenation (i.e., 4 weeks). Error bars are standard deviations around the mean of three replicates.

Figure S4:

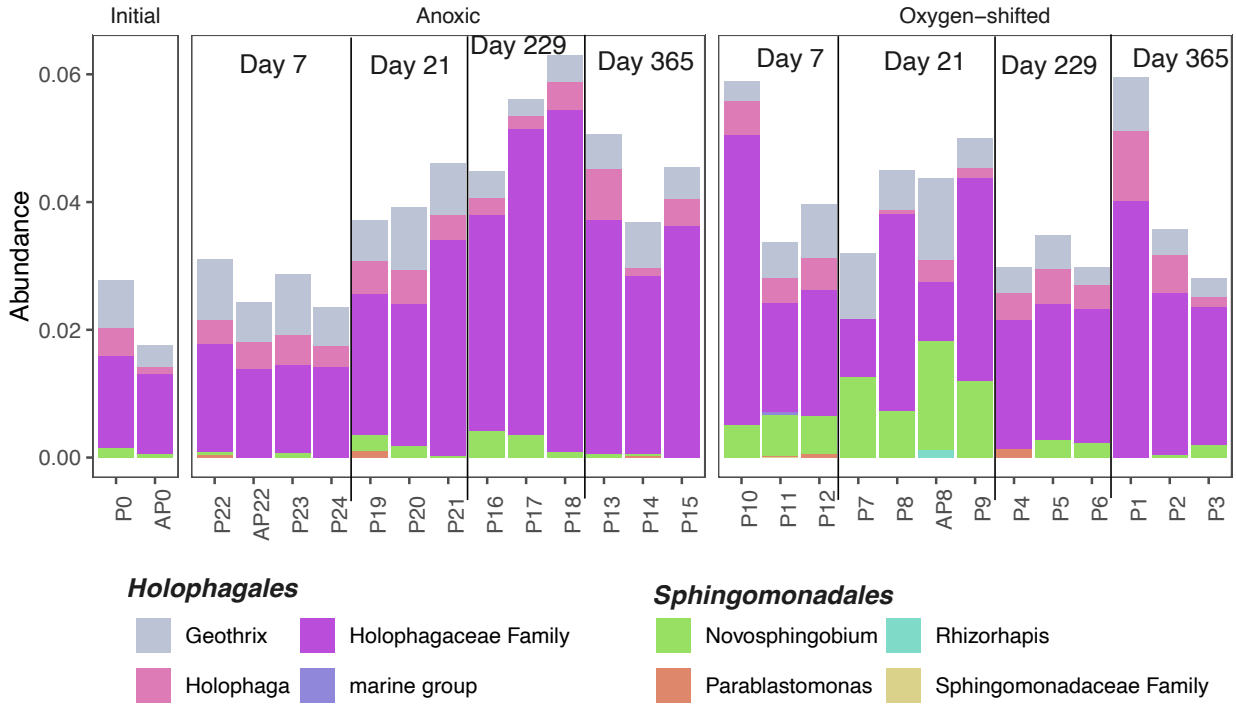

Figure S4: Relative abundance of selected lineages in the PB peat across timepoints. These lineages were identified as key indicator taxa for O_2-stimulation of methanogenesis in the Ward Sphagnum peat.

Figure S5:

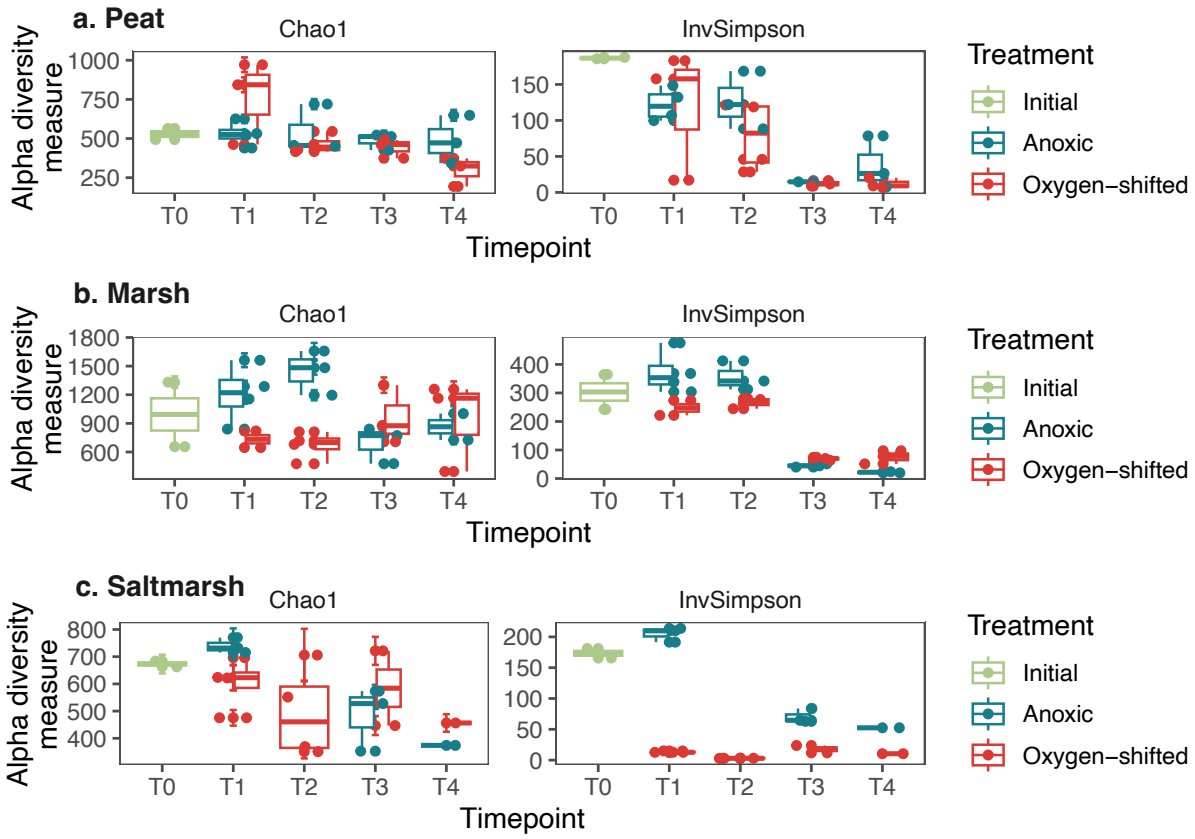

Figure S5: Estimates of microbial community alpha diversity (i.e., Observed number of ASVs and Inverse Simpson index) in the incubations across time for (a) peat, (b) marsh, and (c) saltmarsh. The filtered data used for alpha diversity estimation did not contain singletons. The data were rarefied to even depth before diversity estimation.

Figure S6:

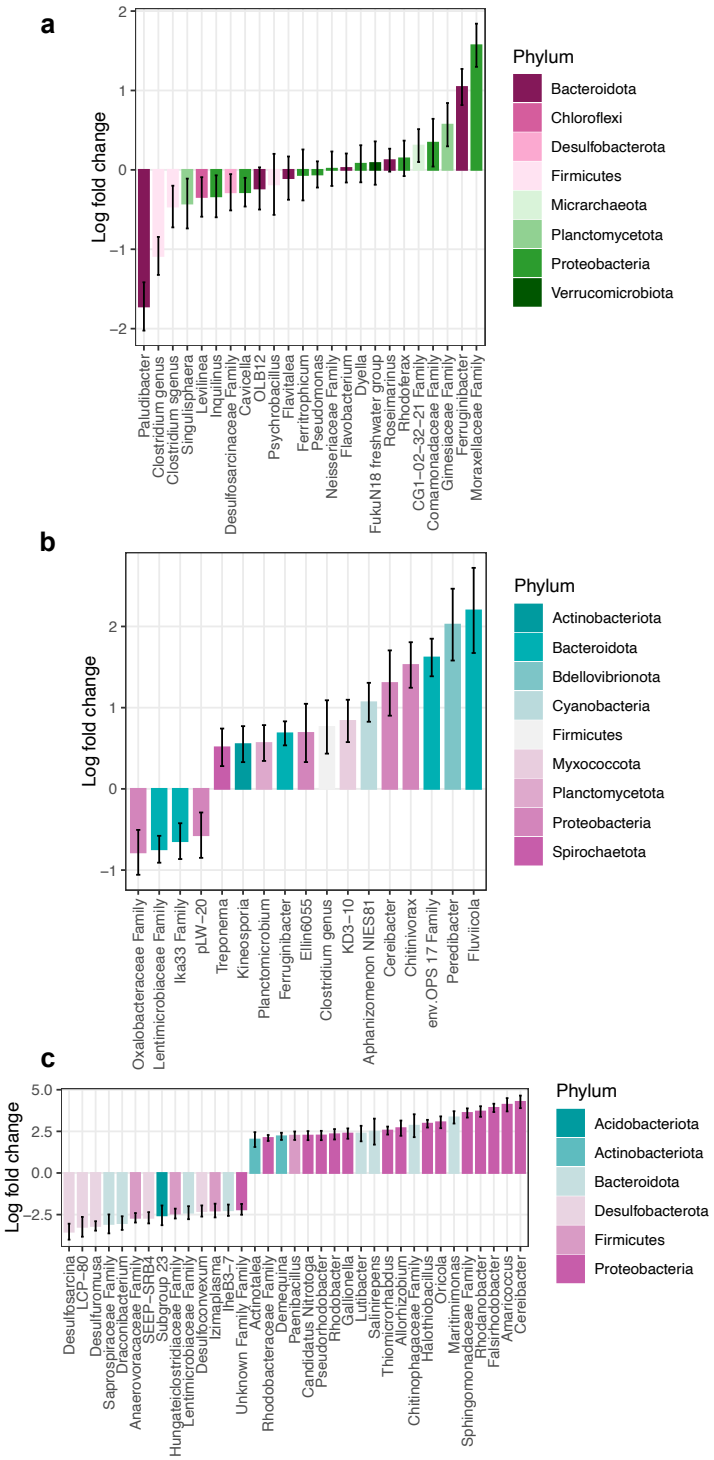

Fig. S6: Summary of the differentially abundant ASVs between treatments in (**a**) PB peat, (**b**) FW marsh, and (**c**) saltmarsh. ANCOM-BC was used for differential abundance analysis. Since

the microbiome changed substantially between treatments for saltmarsh, only those with a fold change of at least 2 are included in (**c**).

Figure S7:

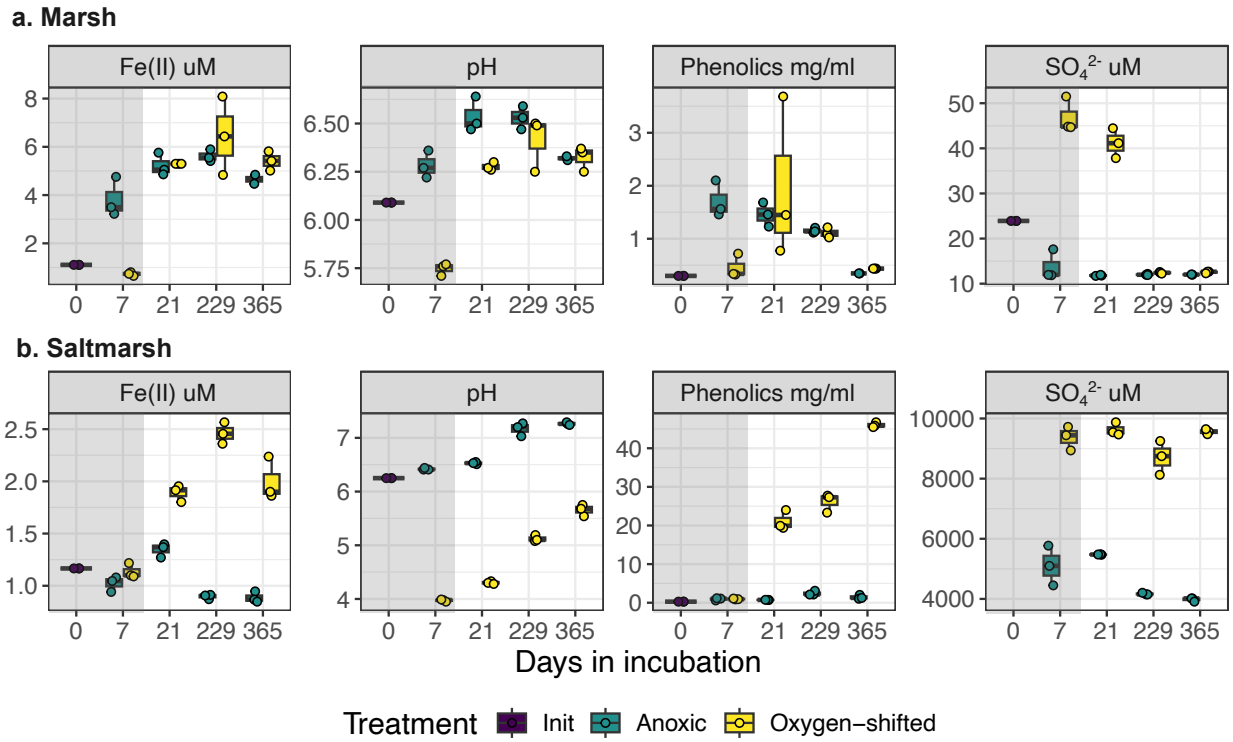

Figure S7: Key geochemical variables measured in FW marsh and saltmarsh incubations across timepoints in the experiment. Oxic period is indicated by the grey rectangles. Three replicate measurements are included in each boxplot (overlayed dots depict the actual values). Phenolics concentrations were measured as mg/ml gallic acid-equivalent.